Rafeindakerfi í skertum víddum í hálfleiðurum

①

- Óvenjuleg hrif
- Tækni, tól

MBE - sameindaúðun

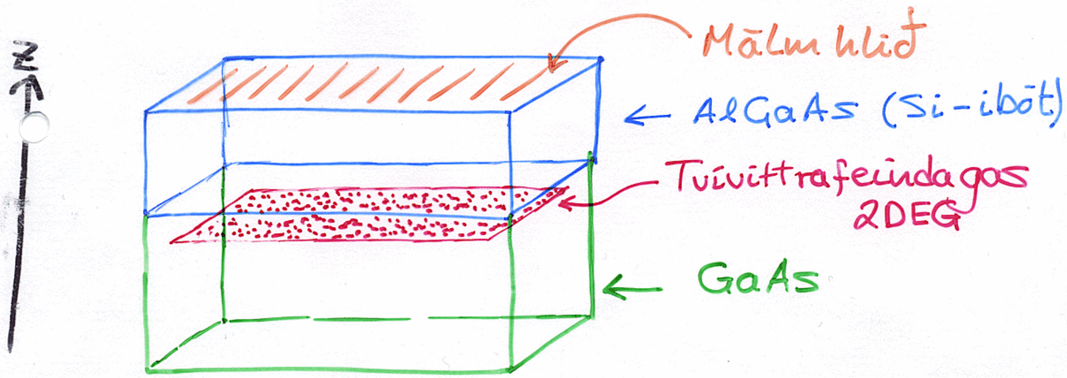

Gegnsær kristallur á innrauða sviðinu

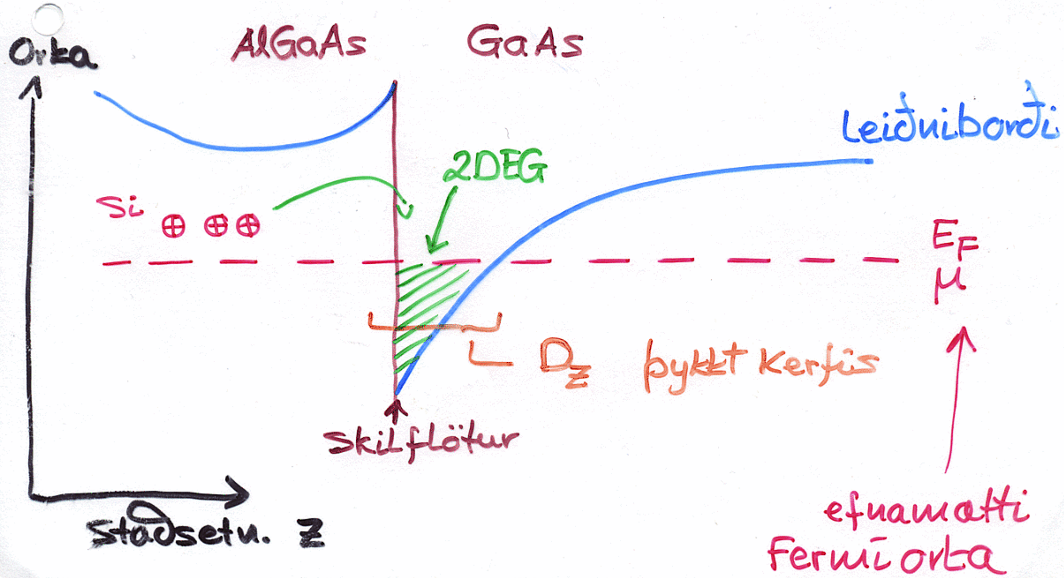

1 Sameindaúðun (MBE)

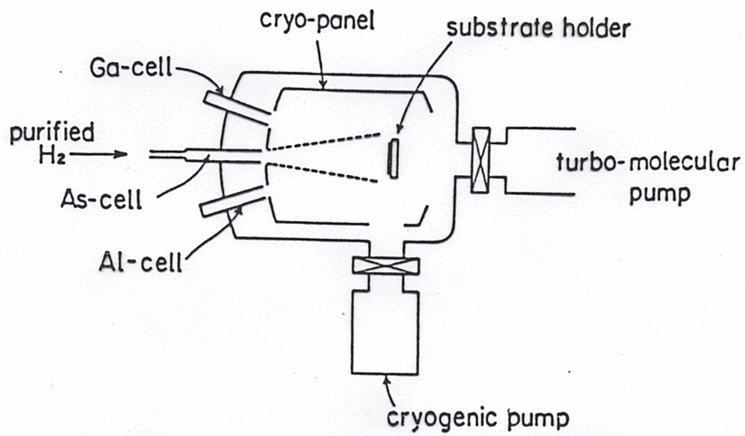

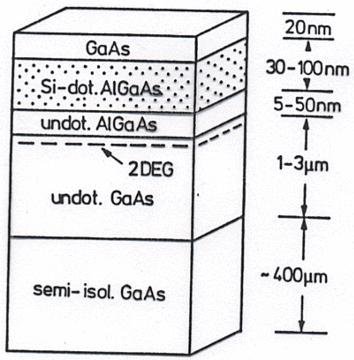

Atom Lasers: The Next Generation

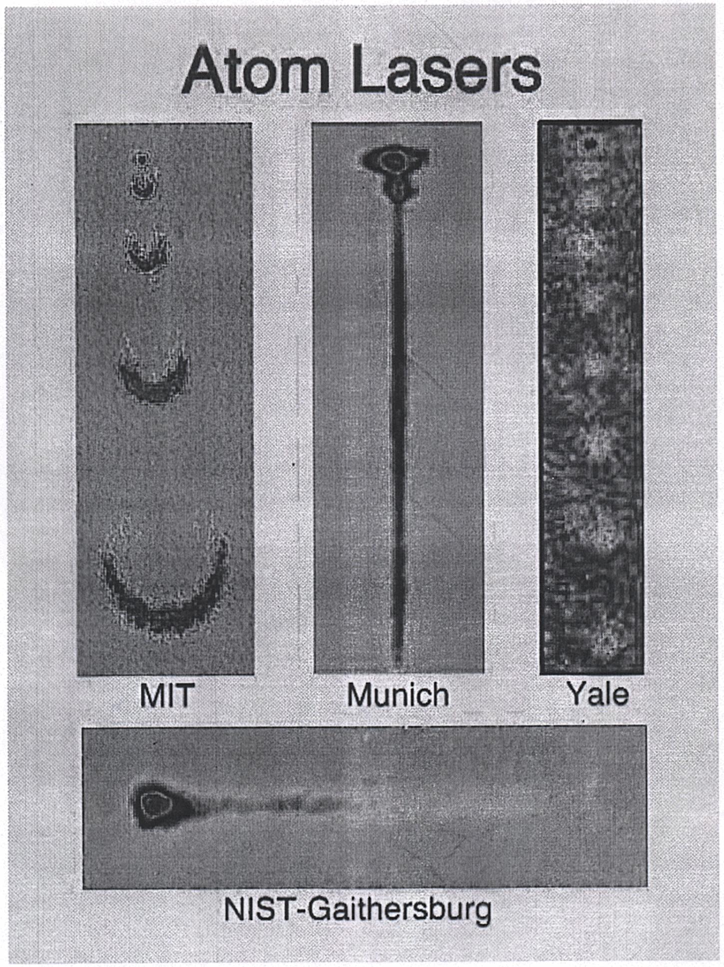

Atom lasers produce highly controlled beams of atoms with desirable properties similar to the light beams produced by optical lasers. The raw ingredients for such devices are ultracold clumps of atoms called "Bose-Einstein condensates," which overlap with one another and fall into the same quantum state, which means that the atoms are highly coordinated with each other. Atom laser devices simply extract beams or pulses of atoms from these BECs.

Frjálsar hreyfingar meðfram skilfleti

Orka ástands merkt með $\mathbf{k}$: $E(\mathbf{k}) = E_z^0 + \frac{\hbar^2}{2m^*}(k_x^2 + k_y^2)$

Skoðum víxlverkun einda síðar

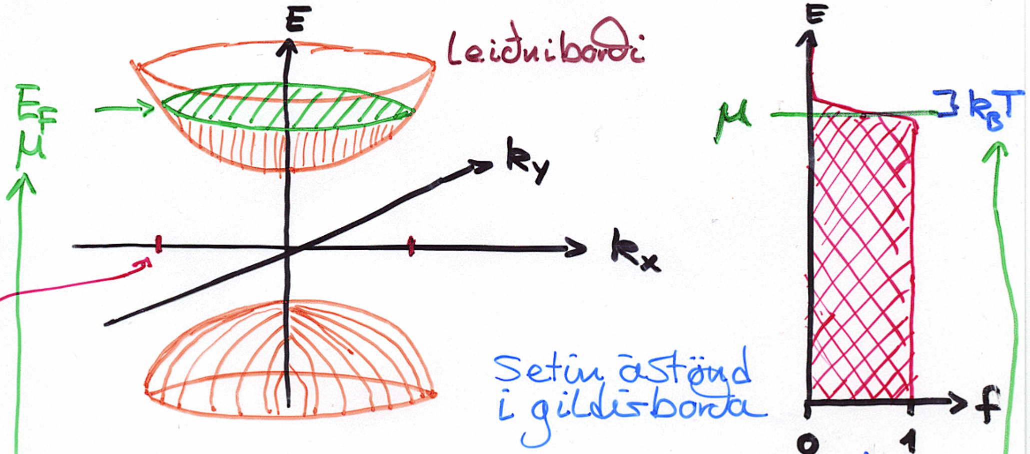

hæstu setin ástönd

hæsti setni bylgjuvigur k_F í leiðniborða

Pauli einsetni Fermidreifing

klassísk varmaorka

Fermi skriðþungi $p_F = \hbar k_F$

Fermi bylgjulengd $\lambda_F = \frac{2\pi}{k_F}$

Ef $\lambda_F >> D_z$ —> 2DEG

Aflfræðilega

1DEG - einvídd

þverskurður

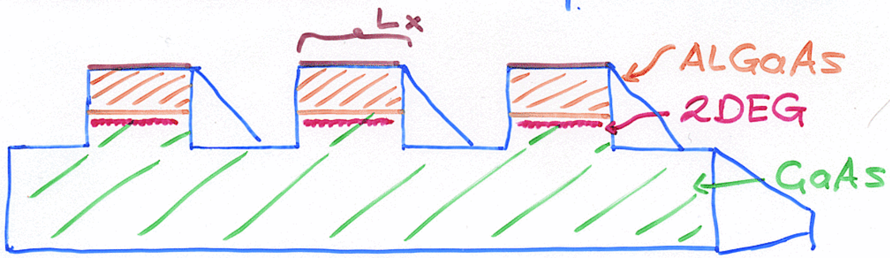

Skammta vírar

$\lambda_F >> L_x$

0DEG

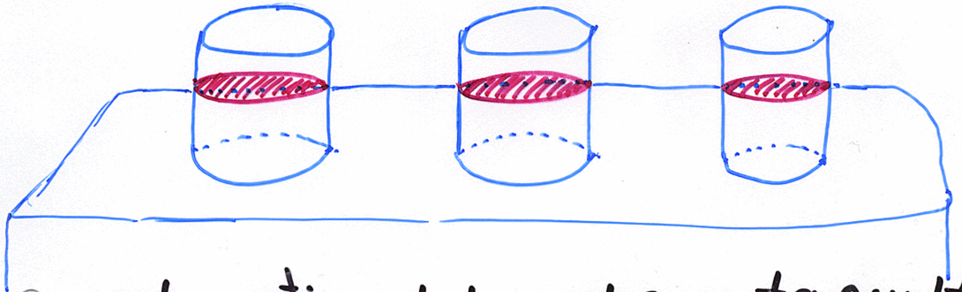

net, raðir stakra skammtapunkta

$\lambda_F >> L_x, L_y, L_z$

Strjál orkustig rafeinda

gervi atóm

Ætt eða mótuð kerfi

atturpunktur

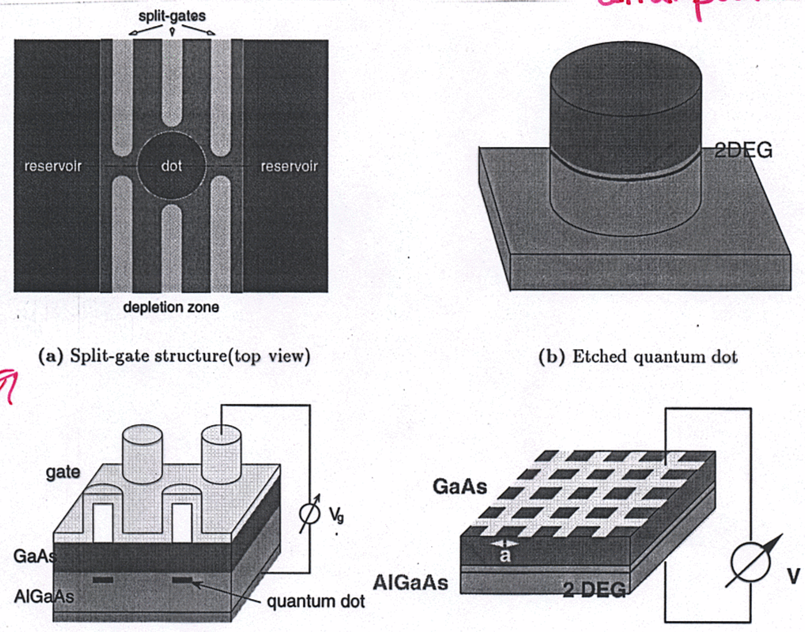

(a) Split-gate structure(top view)

(b) Etched quantum dot

(c) Corrugated gate defining a dot array

(d) Metallic strips defining a superlattice

Fig. 2.2: Different nanostructures.

Kerfi stilgreind með hliði og hliðspennu

Framleiðsla víra

4,2 K werden Beweglichkeiten von mehreren Hunderttausend cm^2/Vs erreicht.

2D-Ausgangsmaterial

Photolithographie und erster Ätzschritt

Teilweise Entfernung des Photolackes und zweiter Ätzschritt

Einlegieren der Kontakte und Wedgen der Probe

Aufbringen von Photolack und Erzeugung von Lackstegen mittels holographischer Lithographie

Aufdampfen des Gates

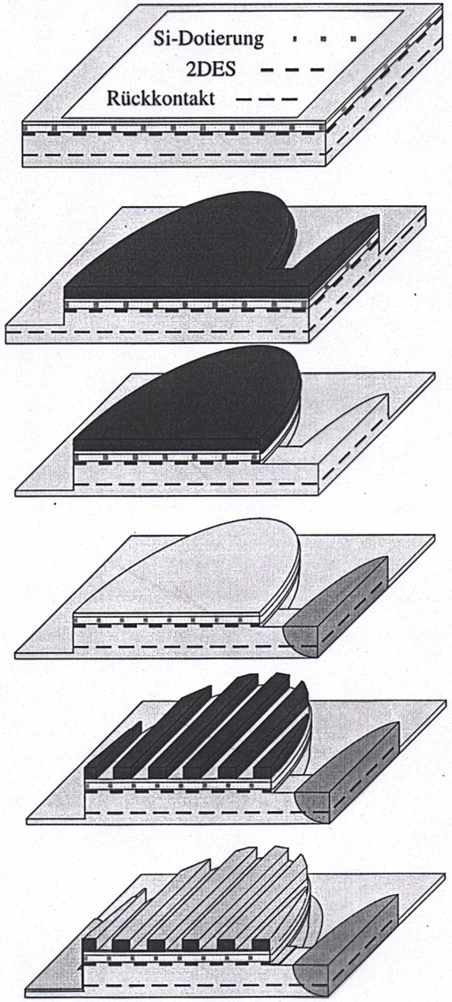

Abb. 2.1: Schematische Darstellung der Prozeßabfolge bei der Präparation von Proben mit Rückkontaktschicht und moduliertem Gate für FIR-Messungen.

Bei der Herstellung von Proben mit Gate bietet sich die Verwendung von Ausgangs-

Grannir skammtavírar

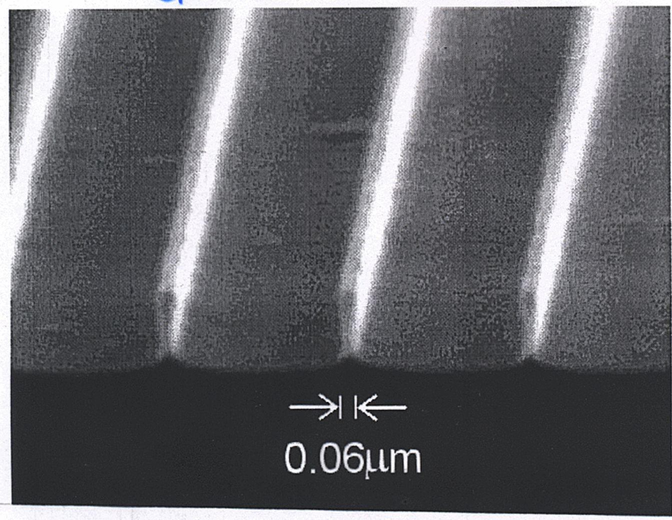

net punkta

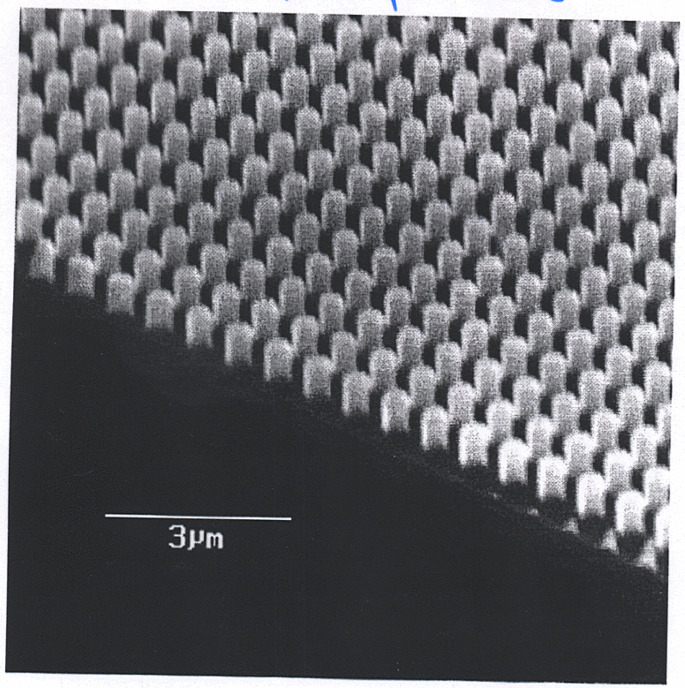

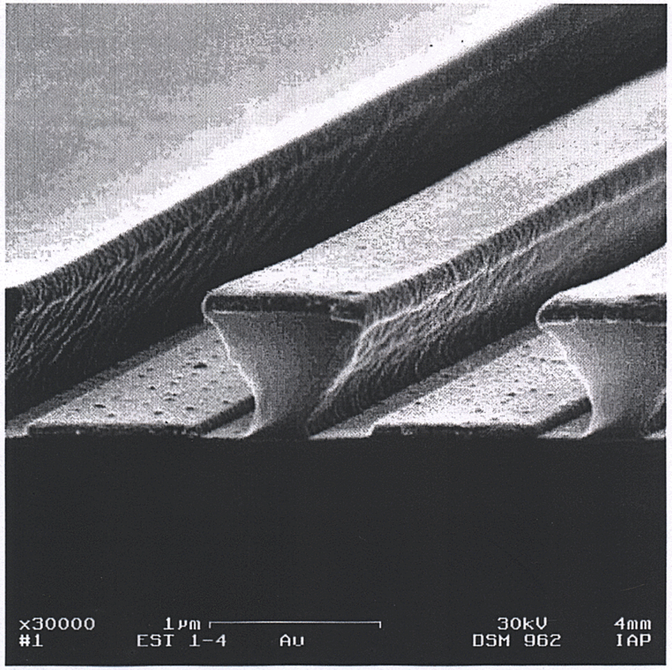

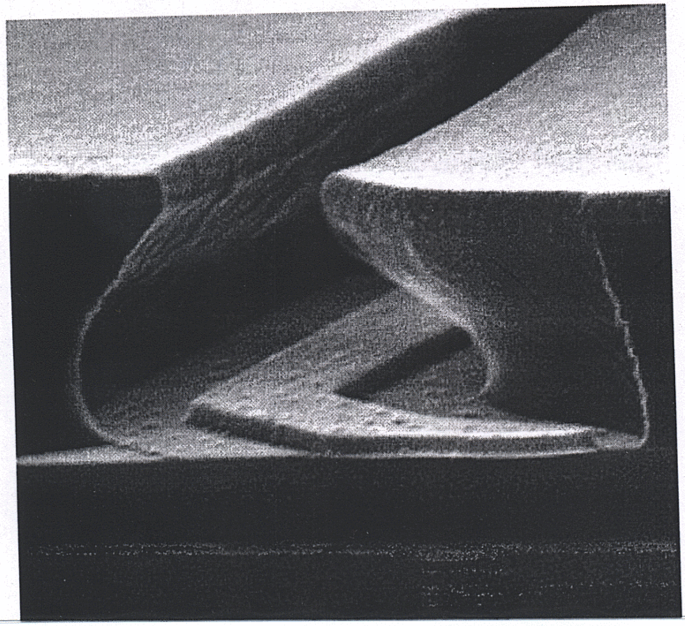

Ástandaþéttleiki DOS

$$\frac{\text{Fjöldi rafeinda ástanda}}{\text{Orkubil} * \text{flatareiningu}} = \text{DOS}$$

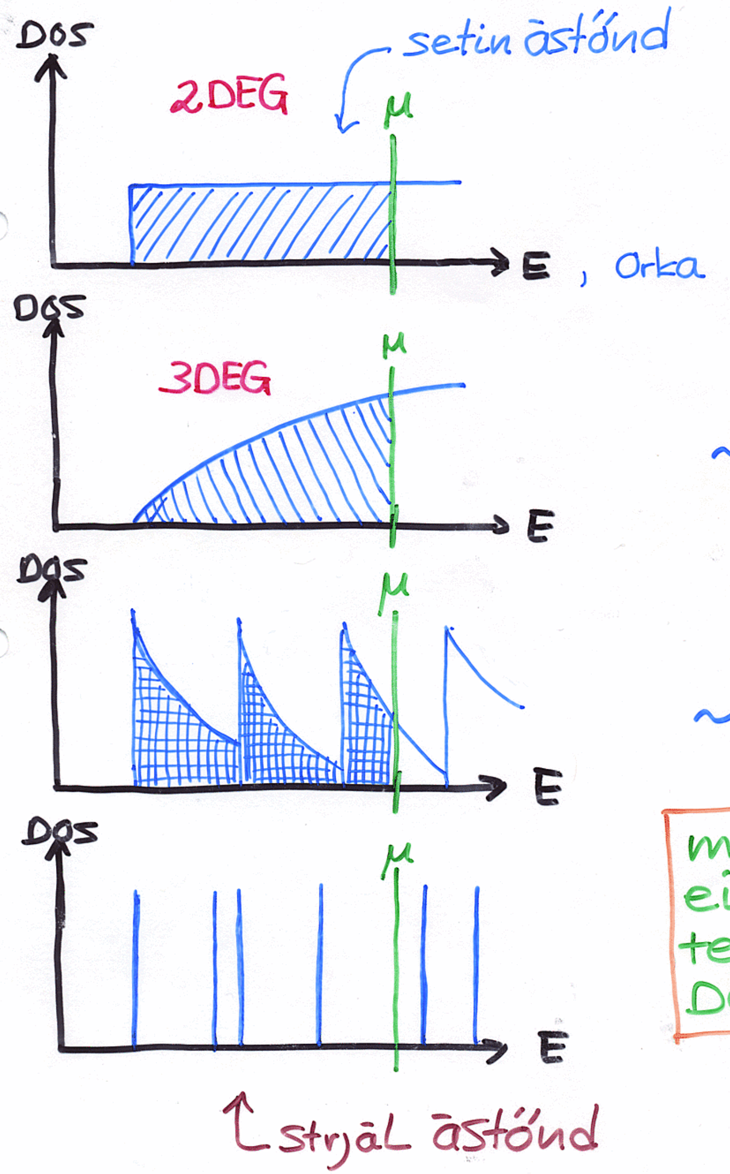

~ fasti

$\sim \sqrt{E}$

$\sim \frac{1}{\sqrt{E}}$

margir eiginleikar tengjast DOS

Hlýgas — Kulgas
2D — 3D

Rafeindagas í hálfleiðara

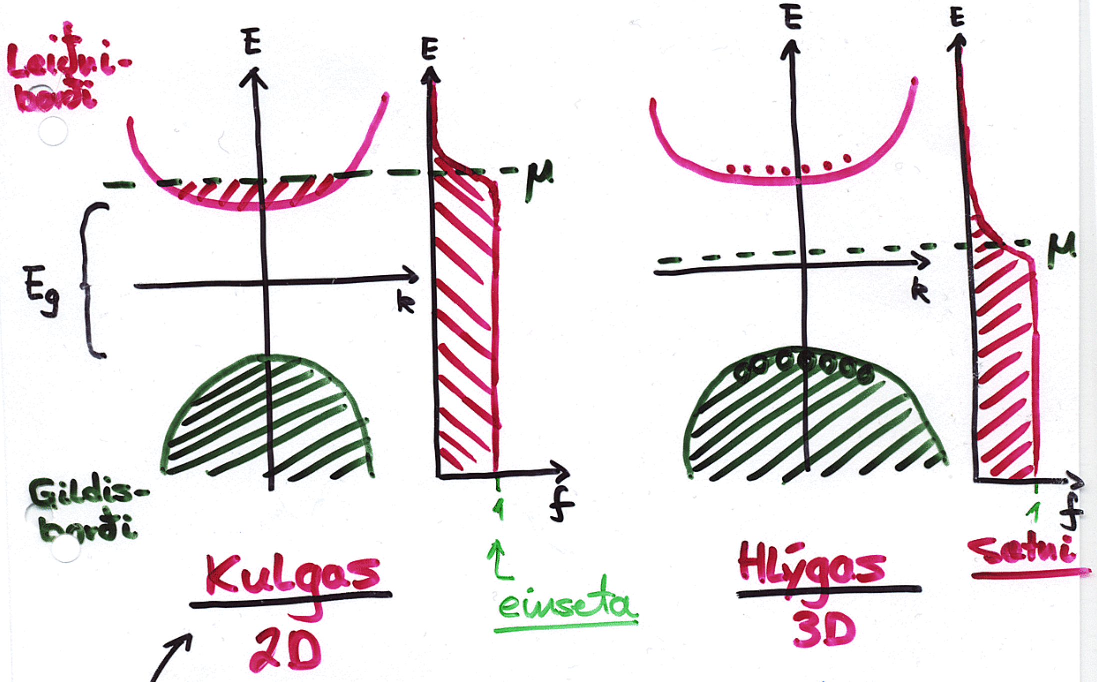

breyta má þéttleikan! ← ekki hægt í 3DEG

Víxlverkun

Coulomb víxlverkun

beinn þáttur

$$V(r) = + \frac{e^2}{4\pi\epsilon_0 r}$$

stöðuorka fráhrinding

skipta þáttur

Fermi eindir með spuna (skammtafræði)

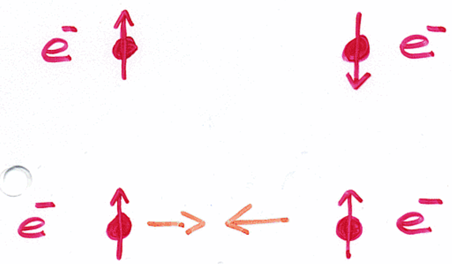

enginn Skiptakraftur

Skiptakraftur aðdráttarkraftur

flókið form (eindir þekkjast ekki í sundur)

en reiknanlegt (óstaðbundið)

2 Skammtafræði

$$(\Delta x)(\Delta p) \geq \hbar$$

Ekki er hægt að staðsetja rafeind nákvæmlega
$\longrightarrow$ líkindadreifing.

Hreyfilýsing fyrir líkindabylgjur
sem ferðast um efnið.

2.1 Orkubrunnur - bundin ástönd

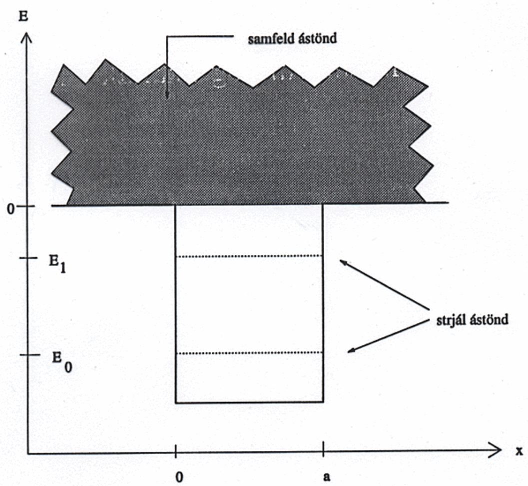

Mynd 1: Orkubrunnur.

Hreyfilýsing

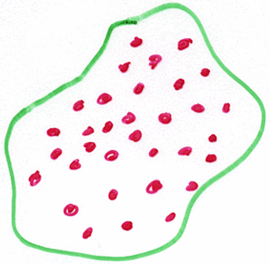

frjálsar eindir
hreyfi orka

$$[H_0 + V]_{ij}$$

víxlverkun

Ummyndun

$$[\mathcal{H}_0 + v]_{ij} \sim [\mathcal{H}_0]_{ij}$$

veik afgangs víxlverkun

frjálsar eindir en hverjar ← **Sýndareindir**

Kerfi		**Sýndareindir**
Rafeindir		
Málmi	→	plasmaeindir
Ofurleiðara	→	Cooperpör
Hálfleiðara	→	plasma. breyttur massi... holur.....
⋮		

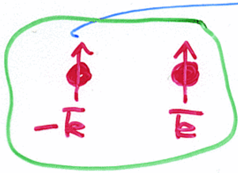

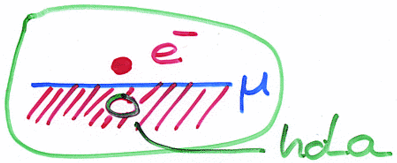

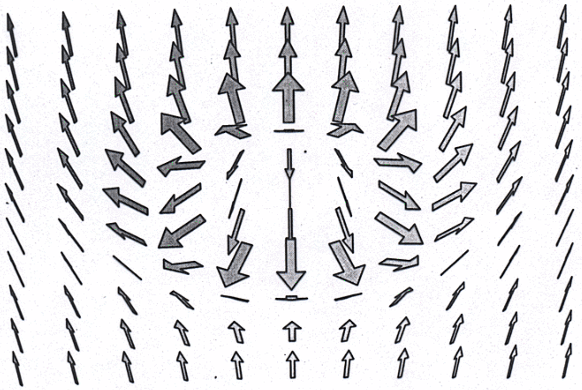

Fig. 9.2: Spin orientation of a skyrmion. The flipped spin sits at its center.

Dæmi um sýndareind:

Skyrmie-eind

Skýling

↕

Lækkun stöðuorku

plasmabylgjur

↕

Hreyfing um jafnvægi

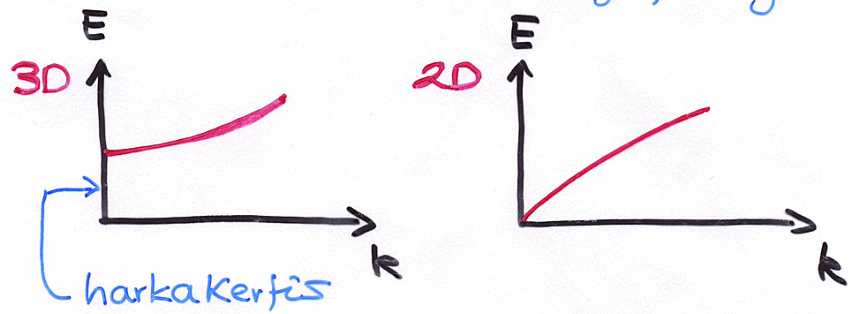

Segulsvið

Lorentz kraftur

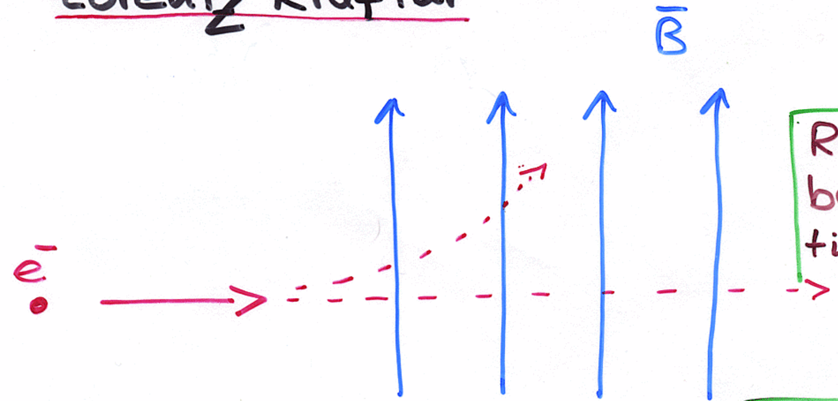

Rafeind beygir til vinstri

↓

Hringhreyfing

$$\bar{F} = +q(\bar{E} + \bar{v} \times \bar{B})$$

Sígild Hall hrif

1879

$$E_x = \rho_{xy} J_y + \rho_{xx} J_x$$

$$E_i = \sum_j \rho_{ij} J_j$$

$$J_i = \sum_j \sigma_{ij} E_j$$

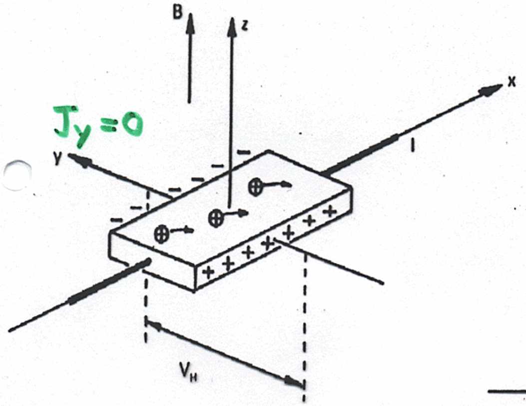

Mælt

$J_y = 0$

$$R_H = \frac{E_y}{J_x B} = \frac{\rho_{yx}}{B} = -\frac{1}{nec}$$

$$\rho_{xx} = \frac{E_x}{J_x}$$

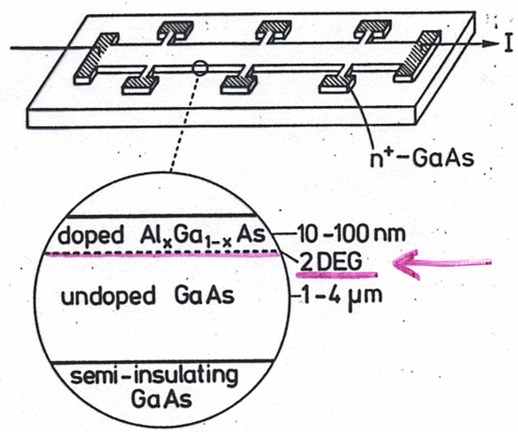

$$\overleftrightarrow{\sigma} = (\overleftrightarrow{\rho})^{-1}$$

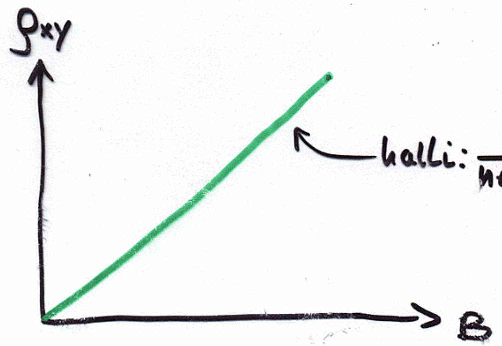

$$\rho_{xy} = -\rho_{yx}$$

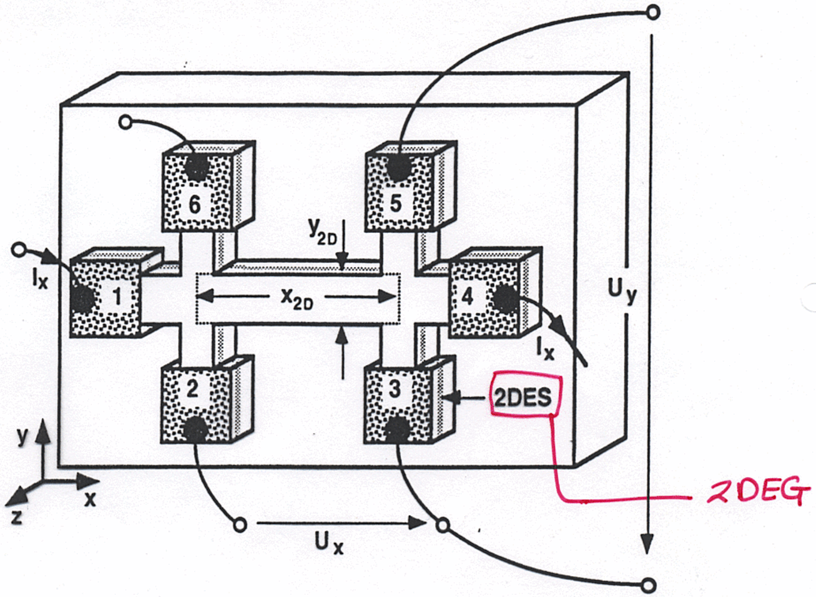

Hall sýni með mælisnertum

③

1980

VOLUME 45, NUMBER 6 PHYSICAL REVIEW LETTERS 11 AUGUST 1980

New Method for High-Accuracy Determination of the Fine-Structure Constant Based on Quantized Hall Resistance

K. v. Klitzing
Physikalisches Institut der Universität Würzburg, D-8700 Würzburg, Federal Republic of Germany, and Hochfeld-Magnetlabor des Max-Planck-Instituts für Festkörperforschung, F-38042 Grenoble, France

and

G. Dorda
Forschungslaboratorien der Siemens AG, D-8000 München, Federal Republic of Germany

and

M. Pepper
Cavendish Laboratory, Cambridge CB3 0HE, United Kingdom

(Received 30 May 1980)

Measurements of the Hall voltage of a two-dimensional electron gas, realized with a silicon metal-oxide-semiconductor field-effect transistor, show that the Hall resistance at particular, experimentally well-defined surface carrier concentrations has fixed values which depend only on the fine-structure constant and speed of light, and is insensitive to the geometry of the device. Preliminary data are reported.

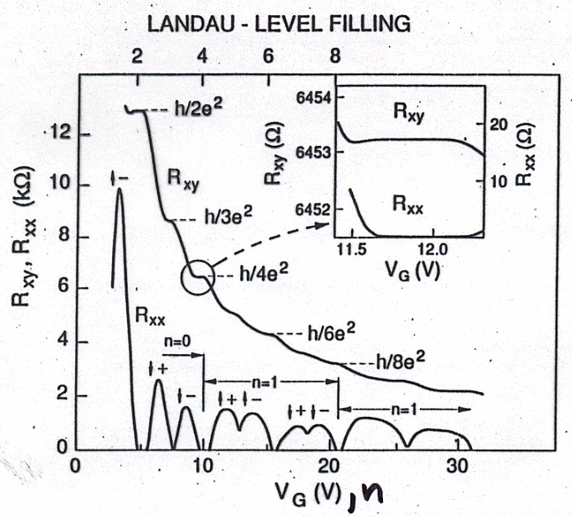

$\rho_{xy} \to \frac{h}{ie^2}$

$i = 1, 2, 3, \ldots$

$\rho_{xx} \to 0$

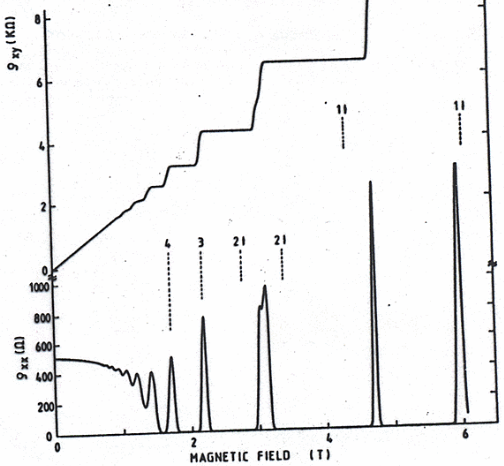

$\sigma_{yx} = i\frac{e^2}{h}$

$\sigma_{xx} \to 0$!

Kawaji

Óhreinindi

nákvæmni

④

Skýring, 2D

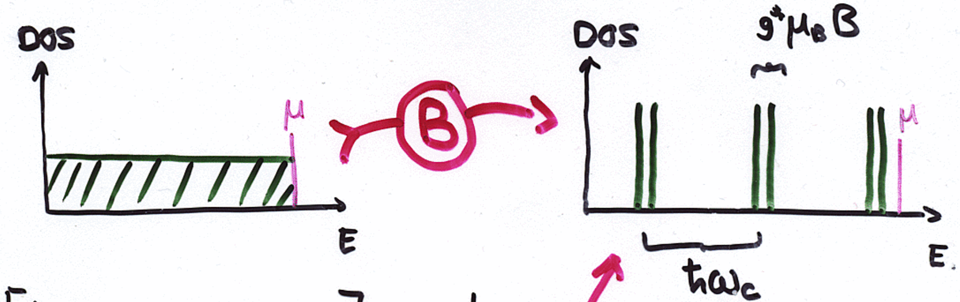

['Ástanda-þéttleiki] = $\frac{1}{l^2 E}$

$\omega_c = \frac{eB}{m^* c}$

Landau-stig

GaAs

$m^* = 0{,}067$

$g^* = -0{,}44$

Hátt B ....

Staðbinding

Margfeldni: $n_0 = \frac{eB}{hc}$

Fylling: $\nu = n/n_0$

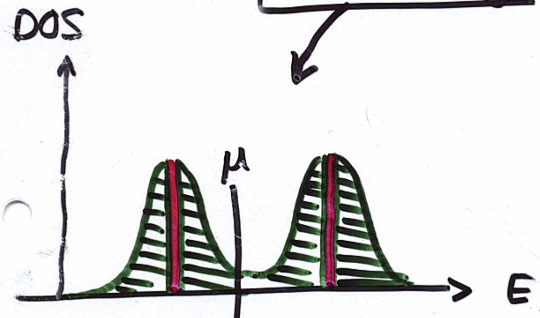

förum μ með B eða n

B ← → n

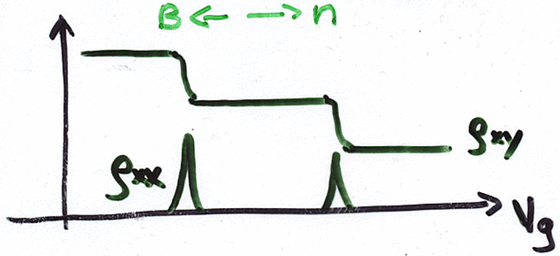

viðnám ↔ leiðni

Staðbinding

2DEG → engin Ohmsk leiðni

smá mottis truflun
→ staðbinding ástanda

Leiðni minnkar með lengd samkvæmt Lografalli

Skammta → staðbinding ← Klassískt

Línulegt í 3DEG <-> Ohm

veldisvísisfalls minnkun í 1DEG

2D, 1D staðbindingar lengd ξ_0

segulsvið dregur úr staðbindingu
Lotubundið

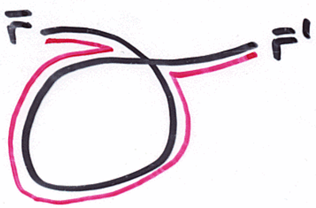

Lokaðar brautir
→ víxlhrif
nād B

Landaustig

$\frac{\hbar^2 k^2}{2m^*}$ → $\bar{B}$ → $\hbar\omega_c(n + 1/2)$

Samf. stig — Segulsvið $\omega_c = \frac{eB}{m^*}$ — Stjál Landaustig

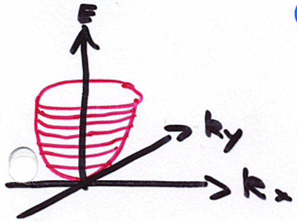

→ B →

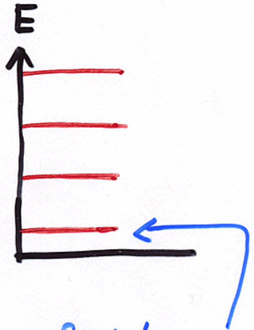

margfeldni

$n_0 = \frac{eB}{h}$

fjöldi ástanda á flatareiningu

segulflæði:

$\Phi = \bar{B} \cdot \bar{A}$

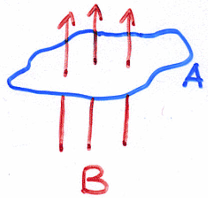

Segulflæðiskammtur

$\Phi_0 = \frac{h}{e}$ → $n_0 = \frac{B}{\Phi_0}$

fylling Landau stigs

$\nu = \frac{n}{n_0} = \frac{N}{A}\frac{\Phi_0}{B} = N\frac{\Phi_0}{\Phi}$: fjöldi rafeinda á fjölda segulflæði-eininga

fjöldi rafeinda

1982 — Wigner 1930 — (5)

VOLUME 48, NUMBER 22 PHYSICAL REVIEW LETTERS 31 MAY 1982

Two-Dimensional Magnetotransport in the Extreme Quantum Limit

D. C. Tsui,[a),(b] H. L. Stormer,[a] and A. C. Gossard
Bell Laboratories, Murray Hill, New Jersey 07974
(Received 5 March 1982)

A quantized Hall plateau of $\rho_{xy} = 3h/e^2$, accompanied by a minimum in ρ_{xx}, was observed at $T < 5$ K in magnetotransport of high-mobility, two-dimensional electrons, when the lowest-energy, spin-polarized Landau level is $\frac{1}{3}$ filled. The formation of a Wigner solid or charge-density-wave state with triangular symmetry is suggested as a possible explanation.

$$\rho_{xy} = \frac{h}{\nu e^2} \qquad \nu = 1/3,\ 2/3,\ \ldots$$

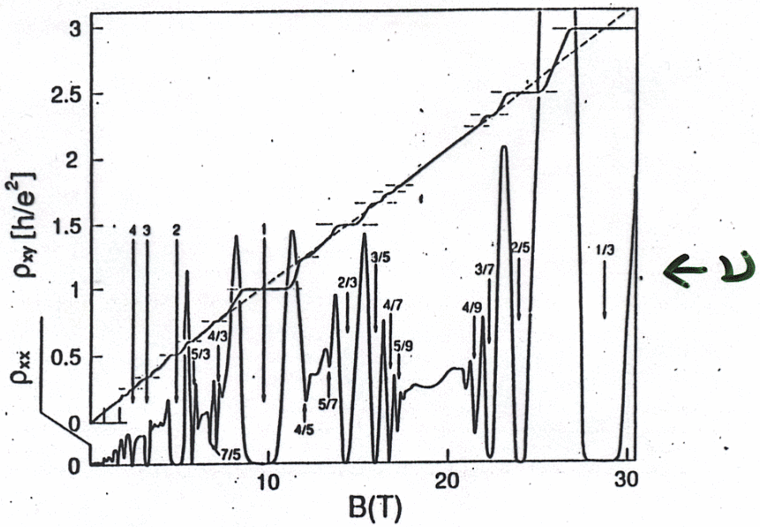

Lægsta Landau-stig

→ $E_{kin} = \frac{\hbar\omega_c}{2}$: fasti

→ áhrif víxlverkunar, !
ekki DOS

Ekki til lítill stiki fyrir truflanaröð ! — (6)

VOLUME 50, NUMBER 18 PHYSICAL REVIEW LETTERS 2 MAY 1983

Anomalous Quantum Hall Effect: An Incompressible Quantum Fluid with Fractionally Charged Excitations

R. B. Laughlin
Lawrence Livermore National Laboratory, University of California, Livermore, California 94550
(Received 22 February 1983)

This Letter presents variational ground-state and excited-state wave functions which describe the condensation of a two-dimensional electron gas into a new state of matter.

Tilgáta um bylgjufall (margeinda)

Vörpun á OCP (Bernstein)
↓
Lægst orka fyrir $\nu = 1/3,\ 1/5, \ldots$
Lægri en fyrir CDW, reynt m. HCA

Búist v. kristöllun f. lægri ν ($< 1/7$)

Örvanir með hleðslu νe !!

Ósamþjappanlegur vökvi

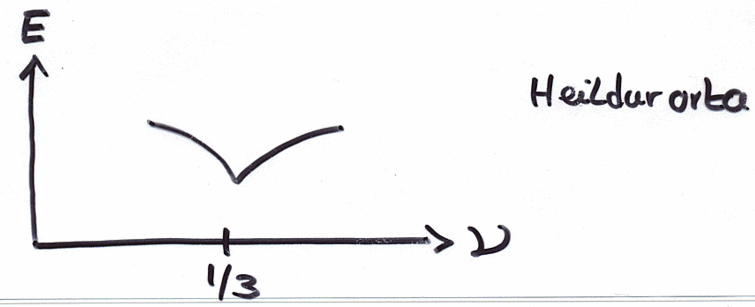

Sýndareindir

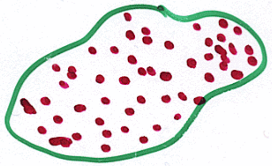

$\{H_0 + V\}_{ij}$ → **ummyndun** → $\{H_0 + v\}_{ij}$

$\sim \{H_0\}_{ij}$

Kerfi	Sýndareindir
Rafeindir	plasmaeindir
	Cooperpör
	⋮

Nóbelsverðlaun 1985 Klitzing

Af hverju einu?

Nákvæmir reikn. fyrir fáar eindir, rétt H

$\{H_0 + V\}_{ij}$ stíft + ~~sett~~ á hornalínu-form

staðfesta hugmyndir Laughlins

Margar hugmyndir

Samsettar fermieindir (CF)

Samhverfa ρ_{xx} í tilraun bendir á sýndareind

$$e^- + 2m\Phi_0$$ ← segulfl. sk.

$m = 1, 2, \cdots$

IQHE ⟷ (Vörpun) ⟷ FQHE

Bein mæling brothleðslu !

Hlustað á suð í mælingum, einstakar eindir .....

$q = \frac{e}{3}, \ldots$

De-Picciotto, R. Reznikov, M. Heiblum, ...
Nature 11. sept. 1997 389 bls. 162

L. Saminad, D.C. Glattli, ...
PRL 29. sept. 1997 79 bls. 2526

Nóbelsverðlaun 1998

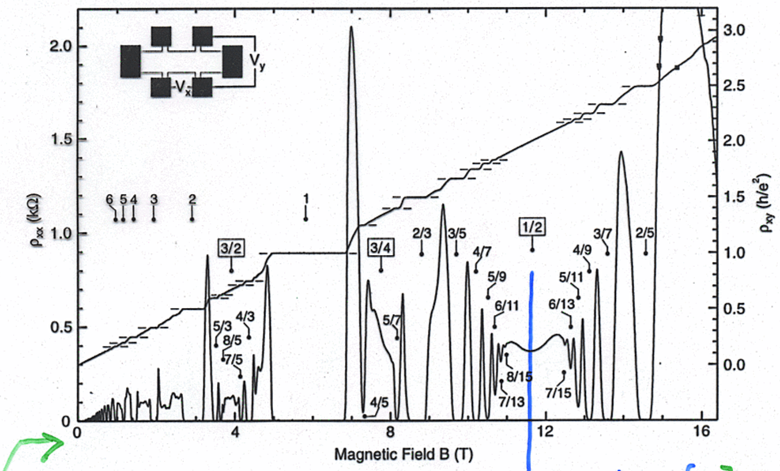

Fig. 15.1: Hall and magneto-resistance of a homogeneous two-dimensional electron system. Numbers indicate the filling factor $\nu = 2\pi\ell^2 n_s$ (n_s: electron sheet density). Courtesy of J. H. Smet.

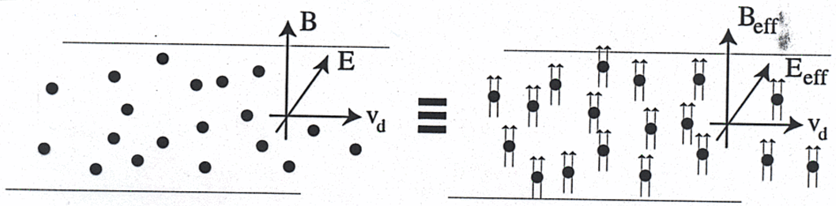

samsettar fermieindir
við $\nu \approx 1/2$
tveir segulflæðistammtar
á eind = Sýndareind
→ $B_{eff} = 0$

Miðsæ rafeindakerfi

Stórsæ kerfi (málmar, hálfleiðarar)

Ófjaðrandi árekstrar rafeinda við veilur og hljóðeindir (mjög tíðir)

↓

brengla innbyrðis fasa rafeinda

meðal vegur milli árekstra l_i

→ klassískt sveim
alger fasa brenglun

Lögun skiptir ekki máli
"Öll sýni eins"

Smásæ kerfi

$L \ll l_i$

engar veilur
samfasa flutningur
leiðni háð lögun

Miðsæ kerfi

$L \approx l_i$

örfáar veilur
lítil fasa brenglun
leiðni háð lögun og staðsetn. veilna

Hreinleiki 2DEG
í GaAs
$l_i \sim \mu m, mm$

Engin tvö kerfi eins

Orkuþröskuldur - smug

Rafeindir geta „smogið gegnum“ þröskuld!

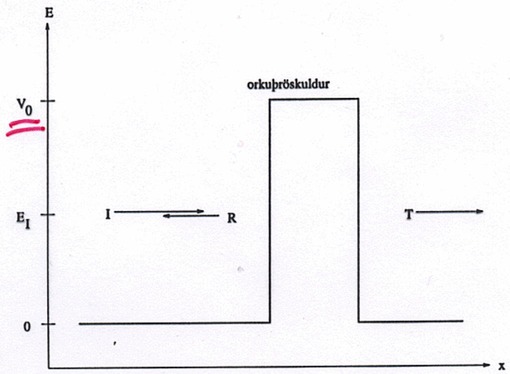

Mynd 2: Smug um orkuþröskuld.

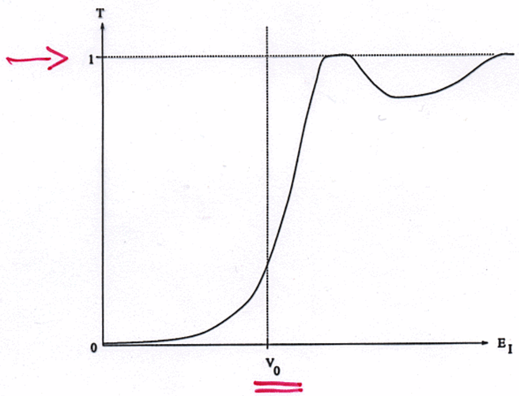

Mynd 3: Líkur þess að rafeind smjúgi gegnum þröskuld.

Hermusmug

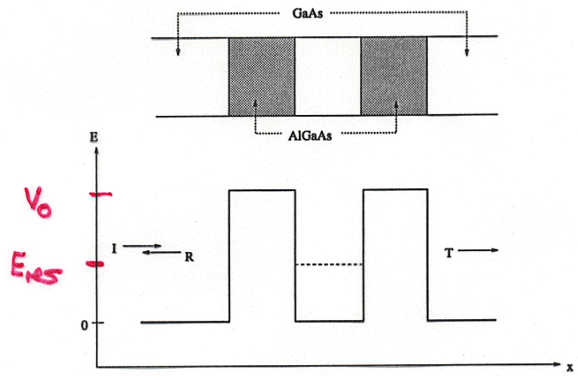

Mynd 7: Smug um tvo orkuþröskulda.

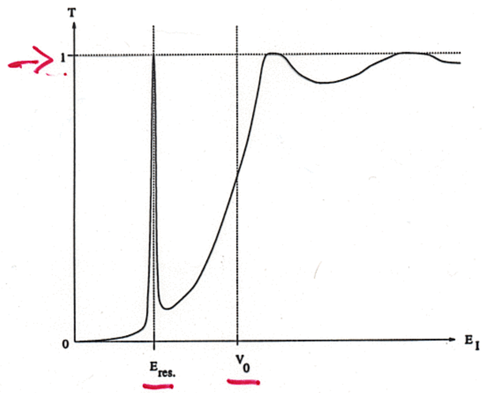

Mynd 8: Líkur þess að rafeind smjúgi gegnum þröskuldana.

Dæmi um smug um einn skammtapunkt

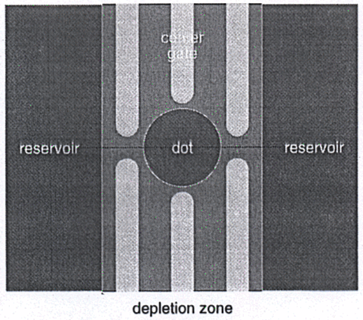

(a) top view

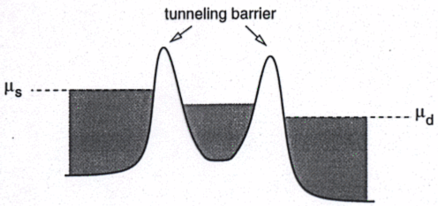

(b) Band edge profile. See also Fig 4.2(b)

Hermusmug

Orkuróf skammtapunkts kannað með smug mælingu

toppar fyrir viðbót rafeinda

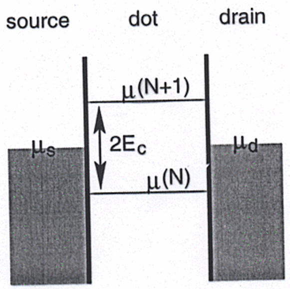

(a) Energy diagram depicting occupied single-particle states in the reservoirs and addition energies of the dot.

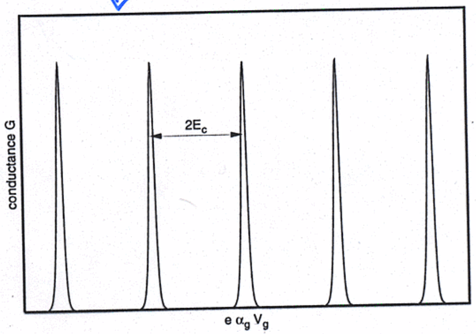

(b) Coulomb blockade oscillations (schematic).

N : fjöldi rafeinda innan punkts

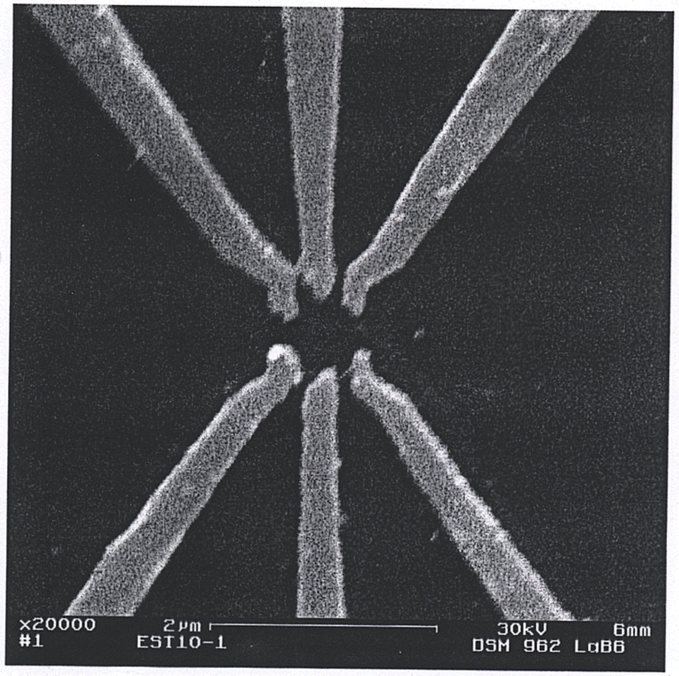

Einstakur punktur skilgreindur með málm hliðum

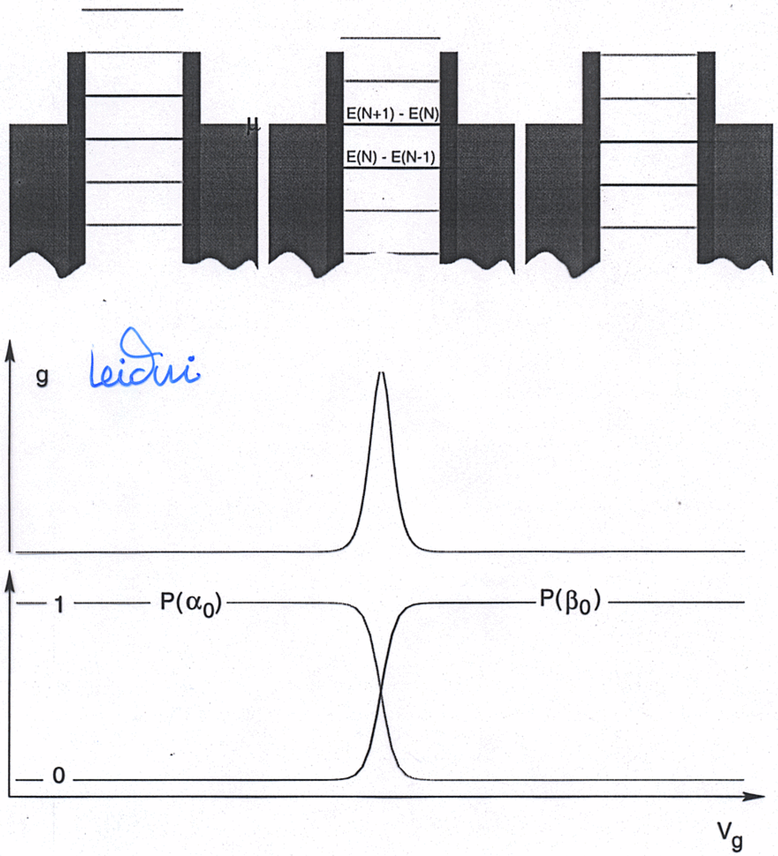

Fig. 11.6: Conductance (middle panel) and ground state occupation probability (lower panel) during the transition from N to $N+1$ particles on the quantum dot induced by an increasing gate voltage V_g. Upper panel: Shift of the quasi-single particle levels $E(N+1) - E(N)$.

Quantum Tunneling Transistor

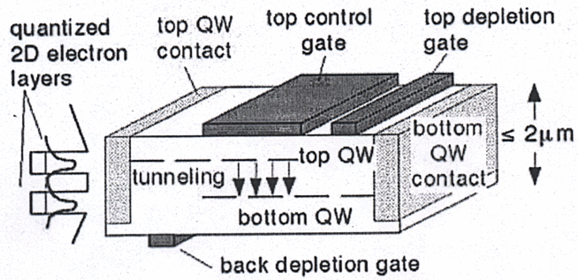

Schematic diagram of a quantum tunneling transistor, an on-off switch that exploits an electron's ability to pass through normally impenetrable energy barriers. The various contacts and gates adjust the voltage between the upper quantum well (labelled "top QW") and the lower quantum well ("bottom QW"), both made of gallium arsenide and having thicknesses of just 150 Angstroms (where 1 Angstrom equals 10^{-10} meters). Adjusting the voltage in the right way allows the electrons in the top QW to "tunnel through" an ordinarily insurmountable barrier (made of aluminum gallium arsenide, depicted as a sawtoothed energy barrier in the leftmost diagram) to the bottom QW. Tunneling occurs when the top QW and bottom QW accept electrons with the same energy and momentum states. (Figure courtesy Sandia National Laboratories)

This research was described at the 1997 IEEE International Electron Device Meeting in Washington, DC, December 7-10, 1997.

Smug um tvo skammtapunkta

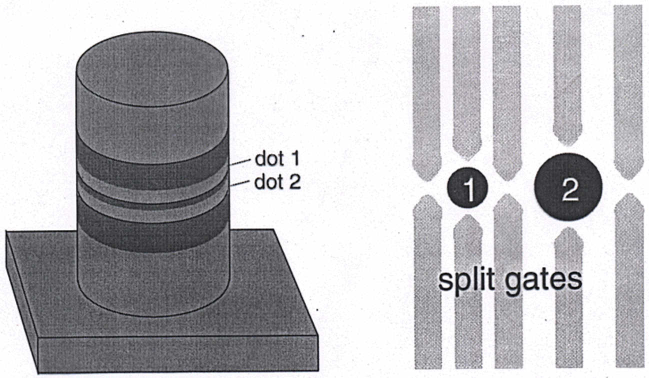

Fig. 12.1: Vertical and lateral double dot structures.

lóðrétt

lárétt

Smug

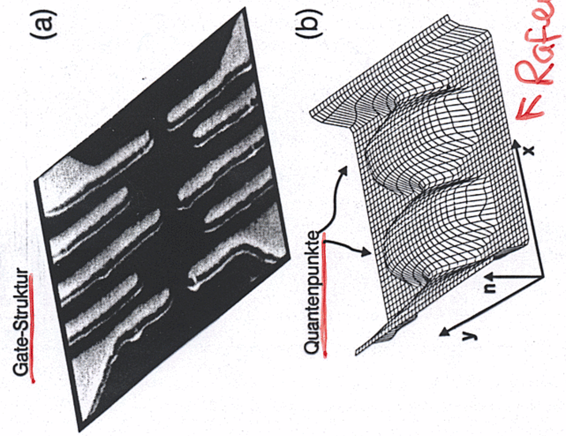

Rafeindaþéttleiki

Abbildung 4.1.2: Ansicht der Gatestruktur eines symmetrischen Doppelquantenpunktes: Rasterelektronenmikroskopische Aufnahme der Struktur (a). Im unteren Teil (b) ist die resultierende Ladungsträgerdichte entsprechend der Geometrie der Mikrostruktur aus (a) dargestellt. Rechts und links befinden sich die Reservoire (2DEG), die linsenförmigen Quantenpunkte liegen, über Tunnelbarrieren angekoppelt, dazwischen. Die Elektronenanzahl liegt hier bei $N = 54 \pm 2$ je Quantenpunkt.

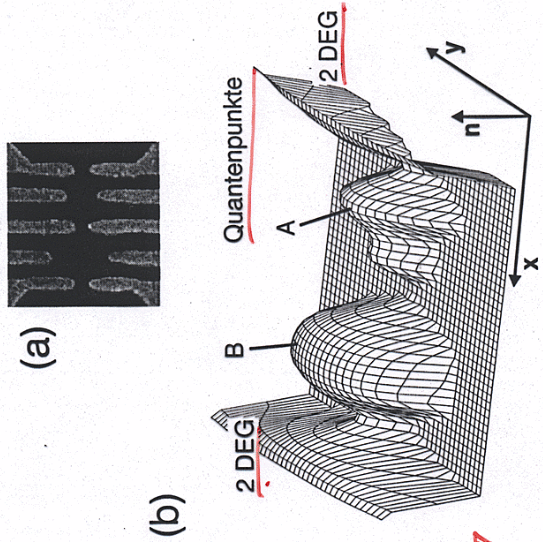

Abbildung 4.1.3: Darstellung des asymmetrischen Doppelquantenpunktes (a). Berechnete Elektronendichte in den Quantenpunkten (b). Der kleine Quantenpunkt zeigt Abweichungen von der gewöhnlichen hemisphärenartigen Gestalt, da die Steuergates dichter am Quantenpunkt liegen.

 Smug um tvopunkta

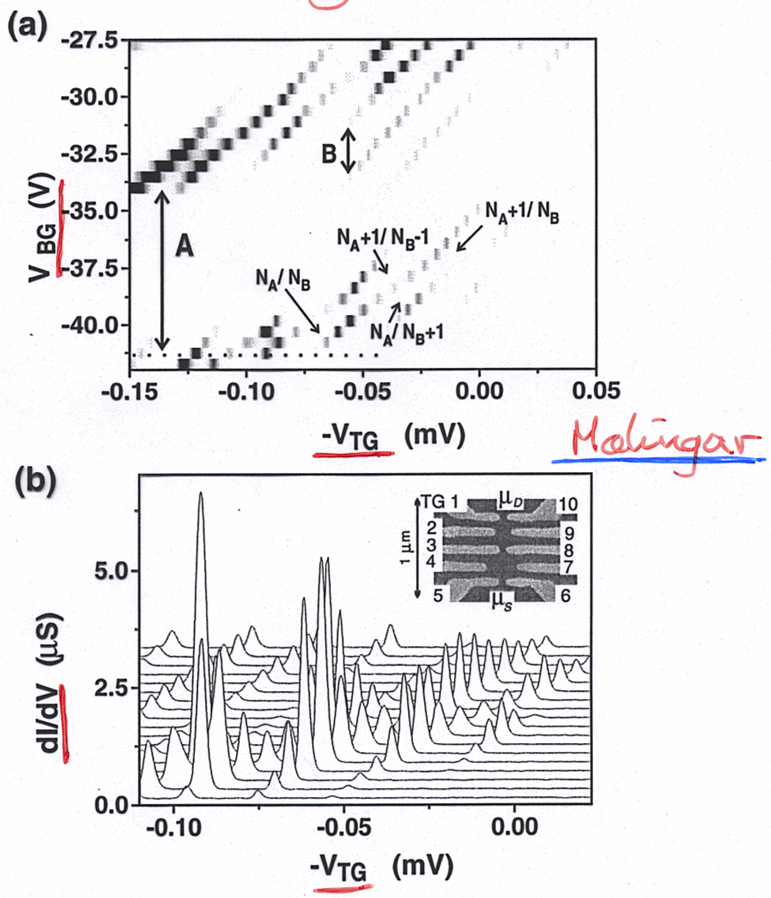

Fig. 12.6: Measured charging diagram of the double quantum dot depicted in the inset. a) The conductance is represented in a gray scale plot - white: $\sigma < 0.5\mu$S, black: $\sigma > 2.5\mu$S. b) Line plot corresponding to the lower part of a). Courtesy of R. H. Blick.

ground state, then, is a superposition of two different ground states with neighboring

Bloch-sveiflur - rafeindatalning

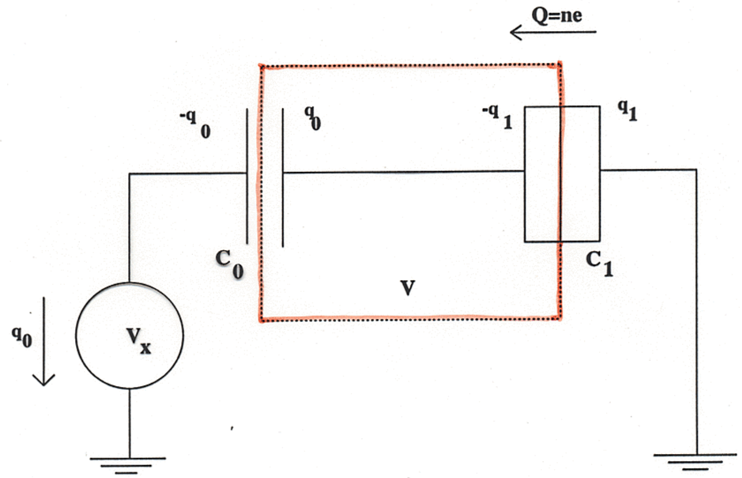

Mynd 4: Rás með örsmáum smugtvisti.

$$E_{ch} = \frac{1}{2C}(Q + q_x)^2.$$

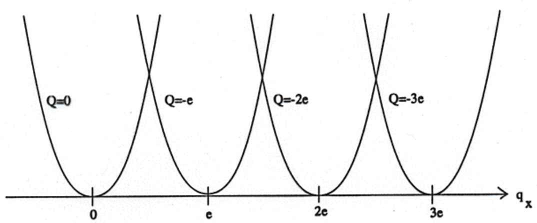

Mynd 5: Stöðuorka rafeindanna í kassanum á mynd 1, sem fall af hleðslunni q_x sem tekin er út úr kassanum.

$$V = \frac{\partial E_{ch}(Q, q_x)}{\partial q_x}$$

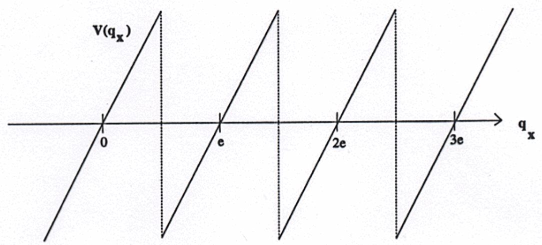

Mynd 6: Spenna þess hlutar rásarinnar á mynd 1. sem er innan strikaða kassans, sem fall af hleðslunni q_x sem tekin er út úr rásinni.

$\Uparrow$

Coulomb-lokun

$\Downarrow$

miljarður skammtapunkta í einu kerfi
hver með nákvæmlega sama rafeindafjölda.

C verður að vera svo smá rýmd að hleðsluorkan fyrir eina rafeind sé $>> k_B T$.

$\sim$ attó farad 10^{-18} C

- **Hermuleiðni**

Leiðni í miðsæjum kerfum er háð lögun kerfis og snertipunkta þess.

Leiðnin er ekki óhmsk, $I \neq \sigma V$.

Hermusmug, Coulomb-lokun.

Athugum líkan eftir K.F. Bergren, eðlisfræðideild Háskólans í Linköping.

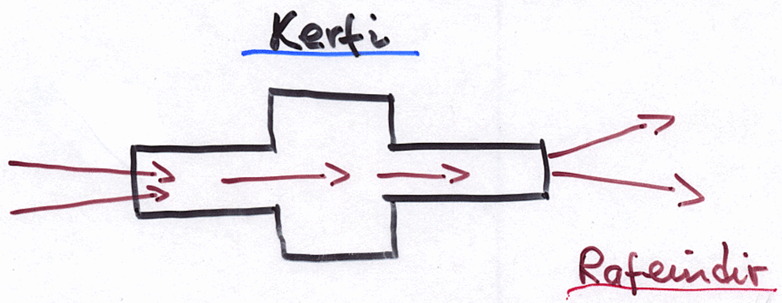

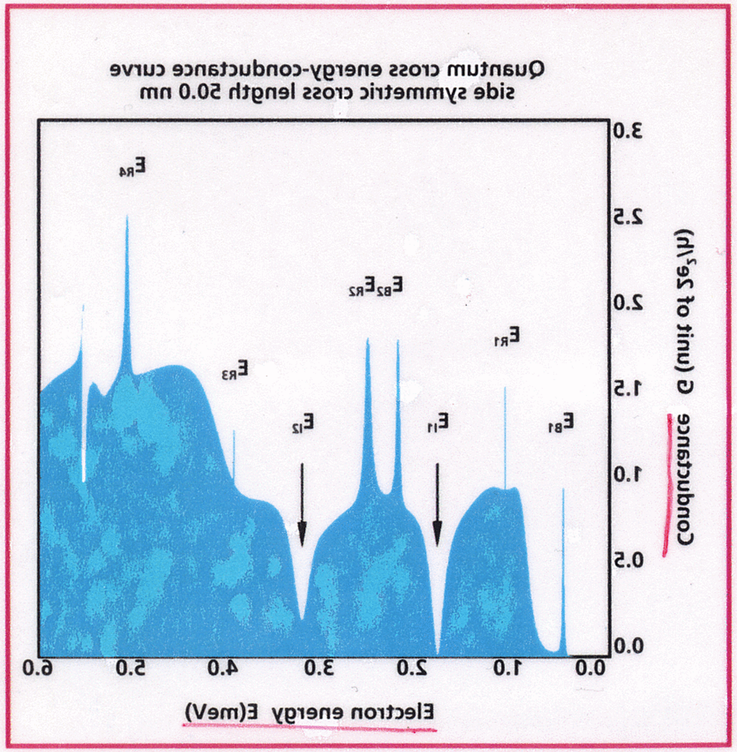

Figure 4. The conductance G at different energies of the carriers for the model quantum structure of Figure 3.

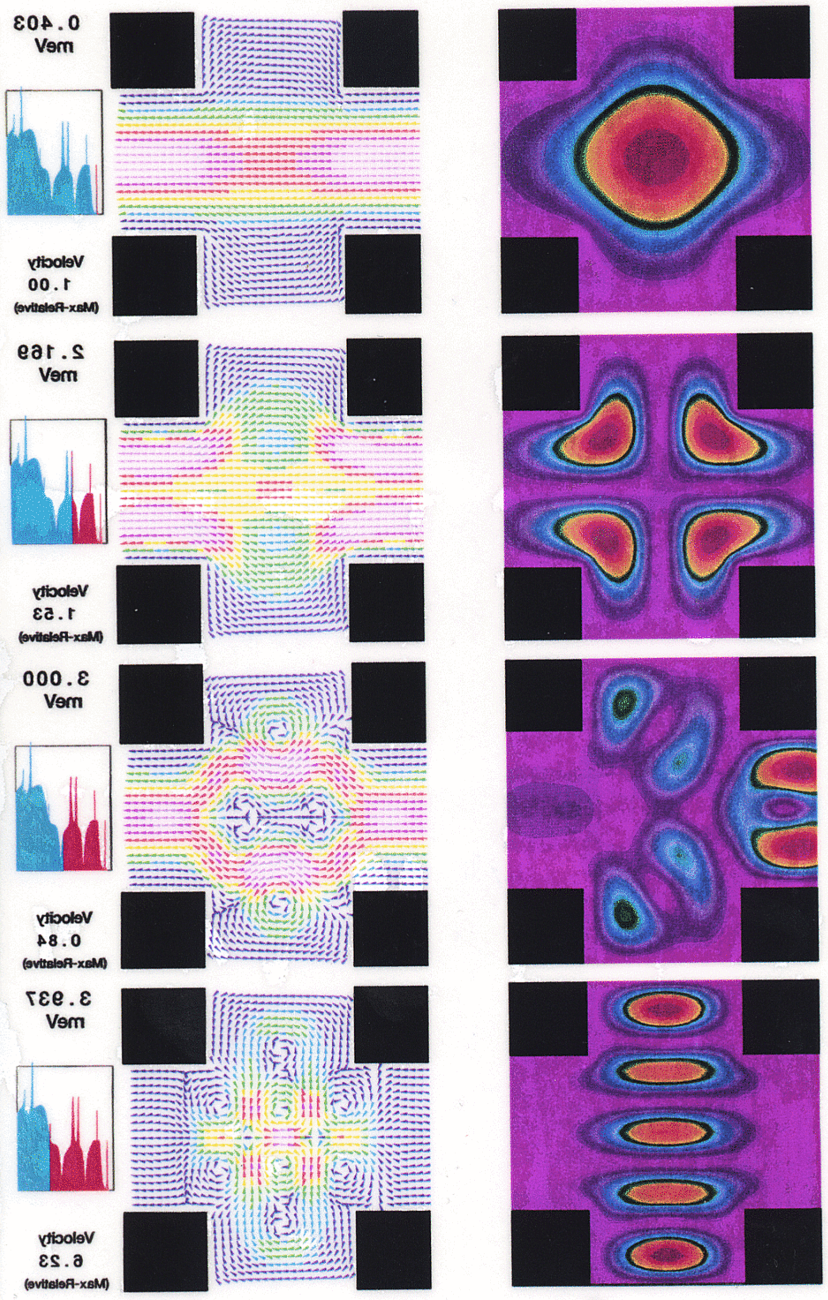

Figure 5. Images of electron and velocity distributions obtained by solving the Schrödinger equation in a model of two interesting quantum channels of finite length. The left column of four pictures shows the contours of electron densities. The highest probability region has been designated as dark red and the lowest region as magenta, by scaling down 45 levels from the maximum relative values: 45.89, 21.94, 5.79, 61.08 from top to bottom pictures, respectively. The middle column shows the associated quantum mechanical velocity distributions where the highest vector velocity has been designated as violet and the lowest velocity as blue, by scaling down seven levels from the maximum relative velocity value as indicated in the right side of each picture. The density and velocity distribution for a given electron energy and its associated conductance has been indicated (red shaded curve) in the right column.

Algilt leiðniflökt í miðsæu kerfi

Segulsvið ruglar rafeindir í miðsæu kerfi

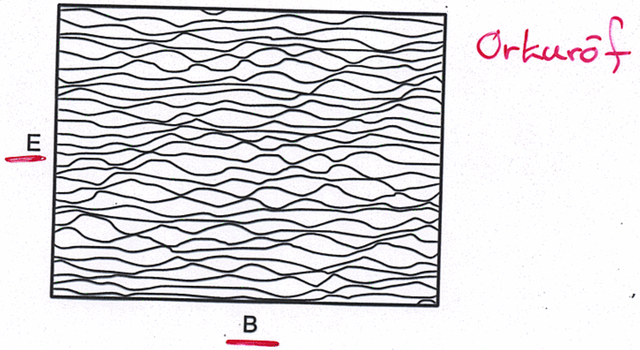

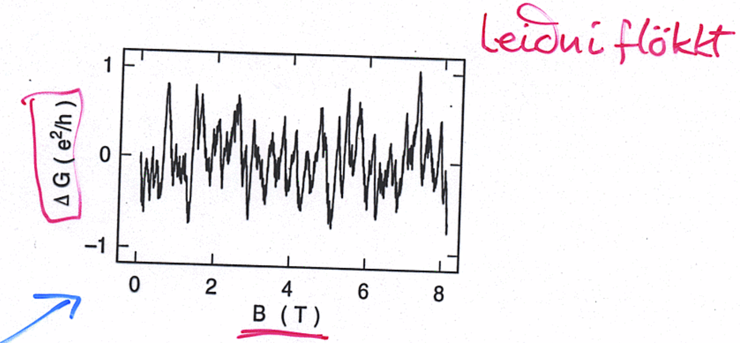

háð kerfi
fingrafar

nákvæmlega endurtakanlegt
stöðugt í tíma

Nanótækni

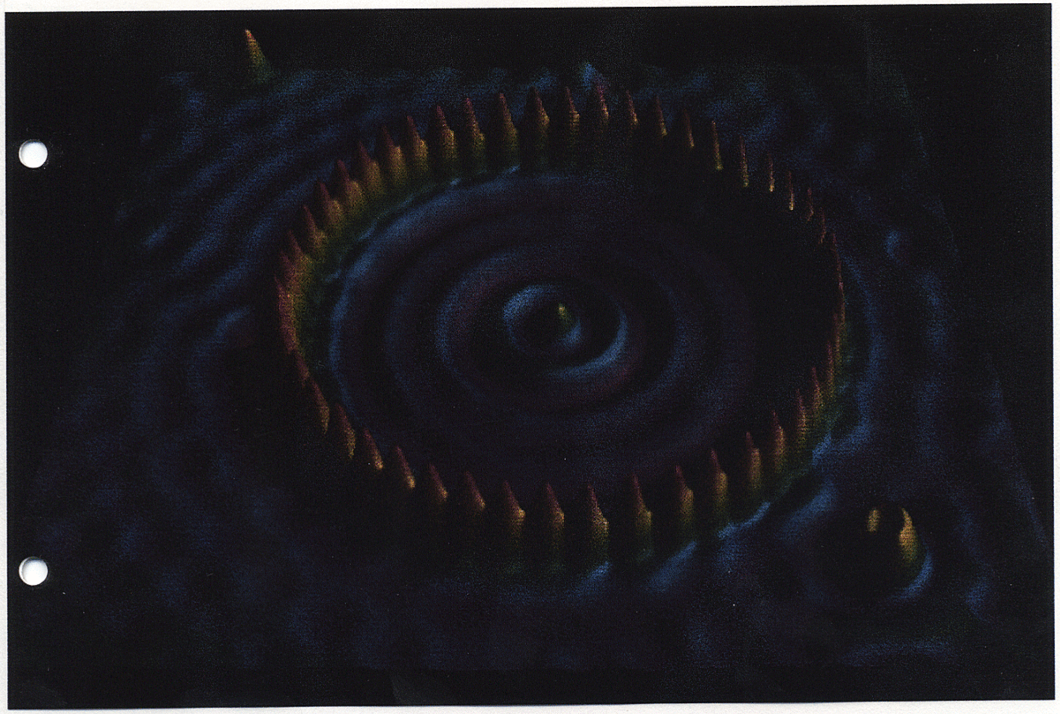

48 járnatóm raðað í hring á koparyfirborði með smugsjá

Quantum Corral

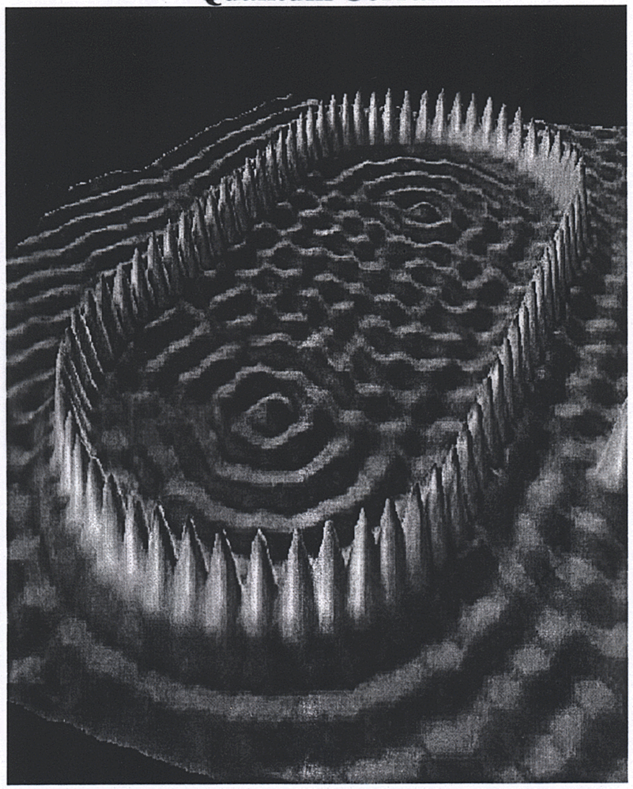

Scanning tunnelling microscope (STM) picture of a stadium-shaped "quantum corral" made by positioning iron atoms on a copper surface. This structure was designed for studying what happens when surface electron waves in a confined region. Courtesy, Don Eigler, IBM.

One Physics Ellipse, College Park, MD 20740-3843
Email: aipinfo@aip.org Phone: 301-209-3100; Fax: 301-209-0843

Aharanov-Bohm-hrif

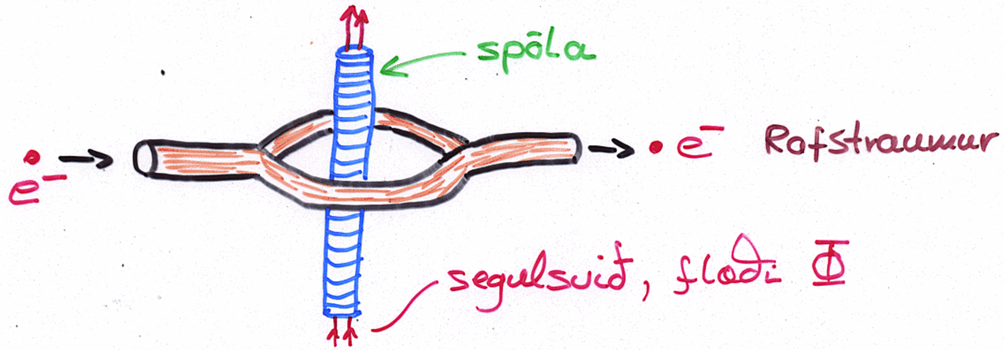

Hálfleiðarasýni

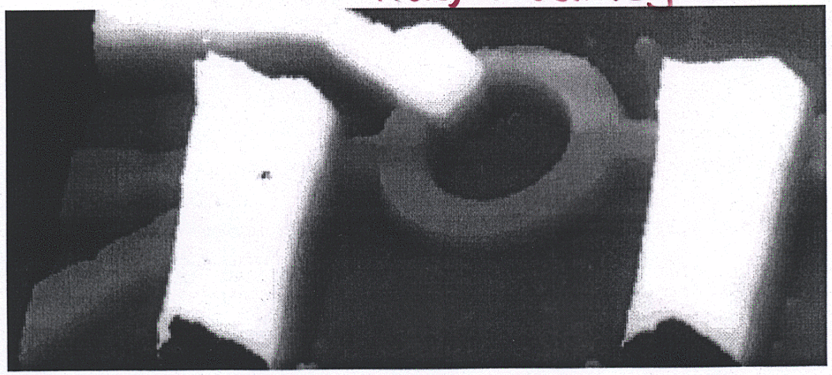

Hreint kerfi → fasi rafeinda brenglast ekki
→ Sístæðir straumar

Breyting á Φ breytir fasa

Styrkjandi og eyðandi víxl.

Leiðni stýrt með segulsviði, rafeindir sjá ekki Φ!

Mæling

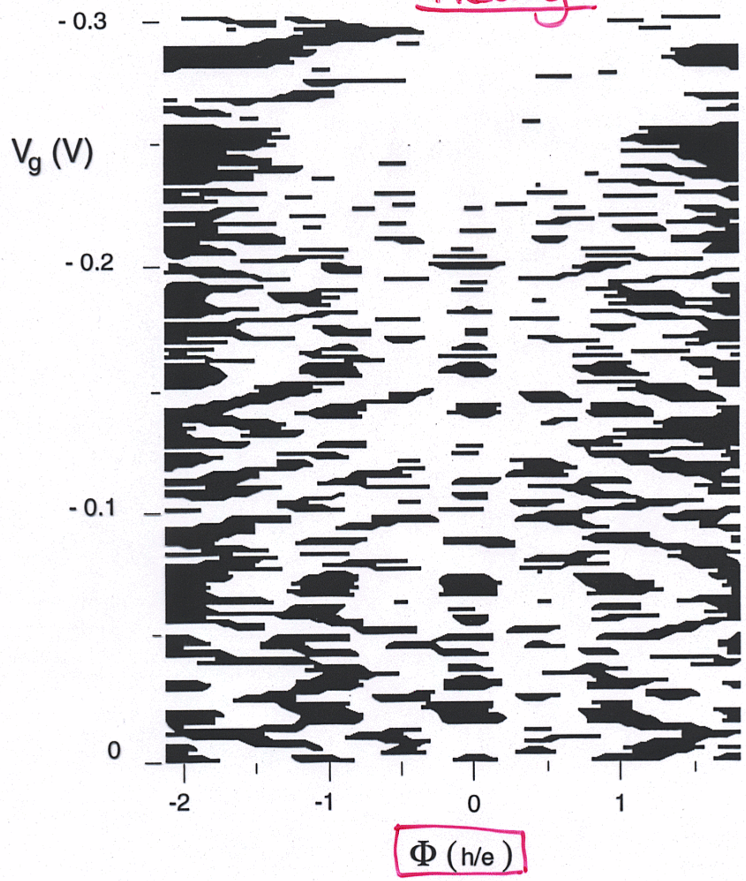

Reiknað

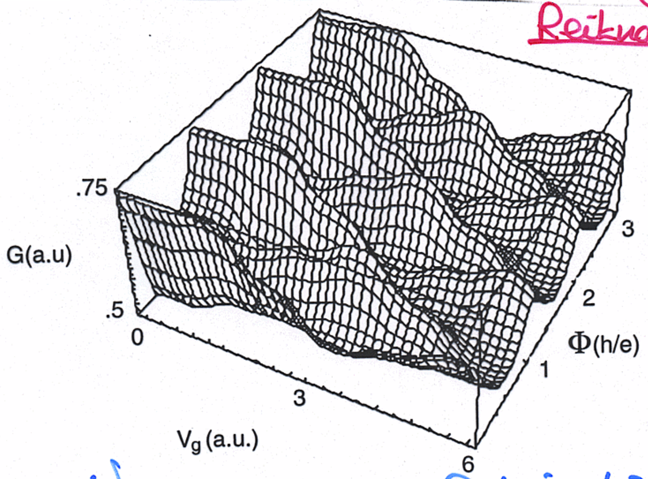

Tengsl við veikingu staðbindingar

Orkuróf skammtapunkts kannað með fjar-innrauðu ljósísogi

Darwin-Fock

Jafnt bil, B = 0, hreintóna sveifill

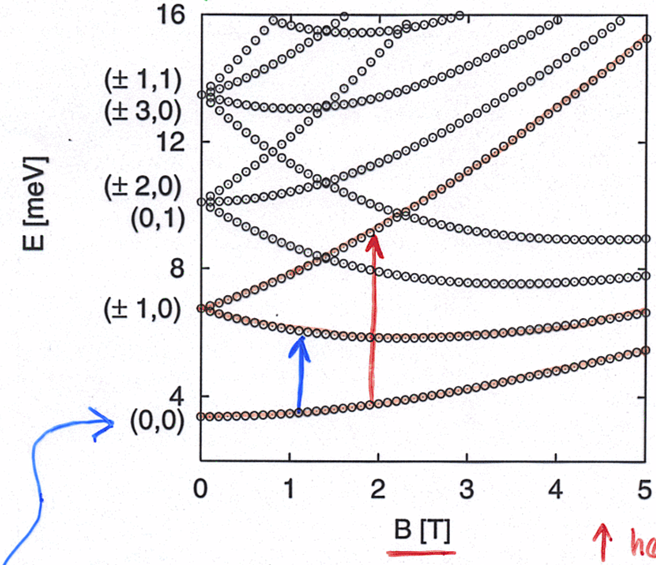

Lb 0

↑ hægri hringskautun

↑ vinstri -||-

(M, n_r)

↑ Skammtatala radíal hreyfingar

↑ Skammtatala hverfiþunga

↑ ↑ mögulegar ljósfærslur einnar rafeindar

$\Delta n_r = 1$

$\Delta M = \pm 1$

tvípólsfærslur

Ljósísog punkts

Hringlaga sporvölulaga

tvísturgröf

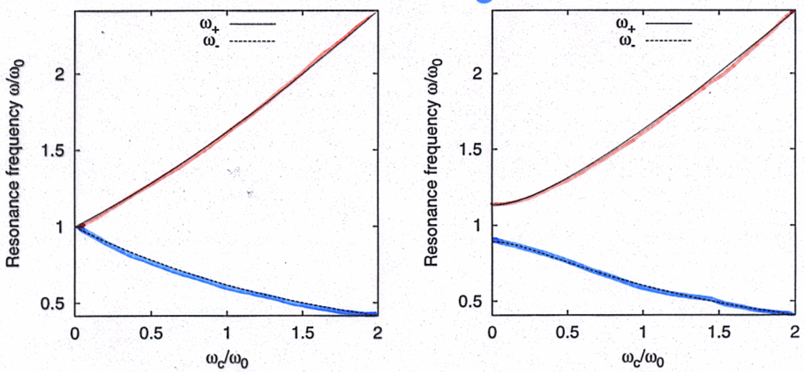

(a) FIR resonances of a parabolically confined quantum dot.

(b) FIR resonances of an elliptic dot with $\omega_x/\omega_0 = 1.05$ and $\omega_y/\omega_0 = 0.95$ (eq. (2.8)).

Ísog óháð N, fjölda rafeinda!

Kohns regla: Ef $\lambda >> L$, fleygboga inni lokun

Ljósið örvar aðeins hreyfingu massamiðju

Engar innbyrðis hreyfingar

ísogs tíðni $F\left(\frac{Q}{M} = \frac{-Ne}{Nm}\right)$ eins og fyrir eina eind

Heildarorka rafeinda í fleygboga skammtapunkti

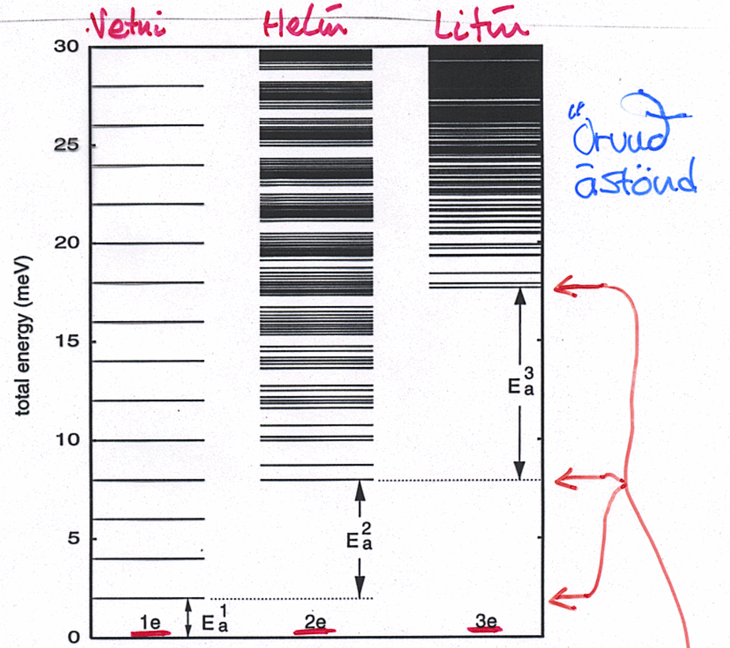

Fig. 11.4: Spectra of QD-hydrogen, QD-helium, and QD-lithium at zero magnetic field. Arrows indicate the addition energies $E_a^{(N)} = \mu(N)$. Parabolic confinement, $\hbar\Omega_0 = 2\text{meV}$, GaAs parameters, $\hbar\Omega_0/Ryd^* = 0.34$. From [349].

Grunnástand

Nákvæmir reikningar

Kassalaga innilokun

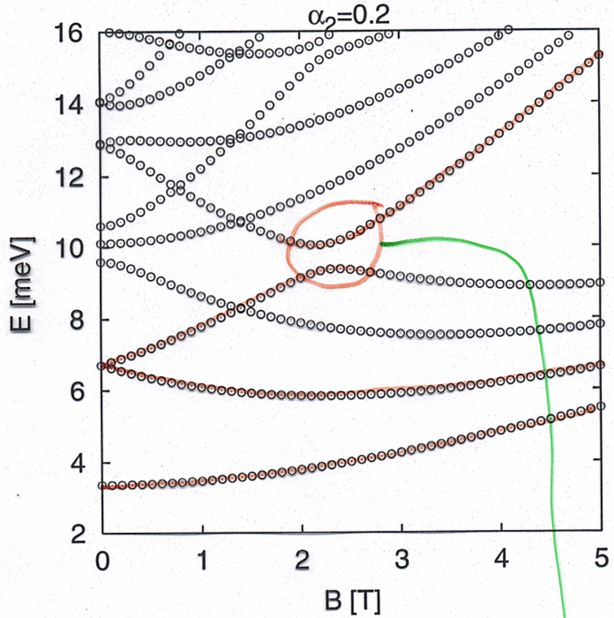

Darwin-Fock

Ein eind eða massamiðja

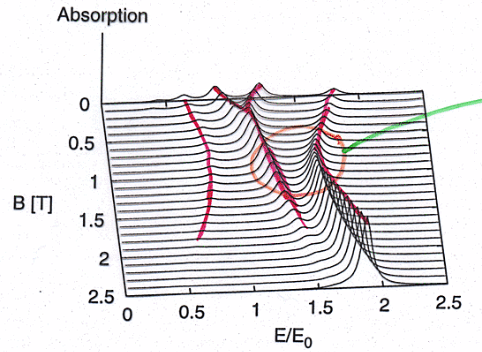

endurspeglast í ísogi

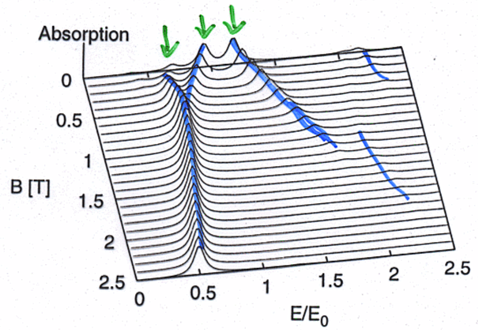

ísogslínur fyrir innri heyfinga- sjást

Ljósísog

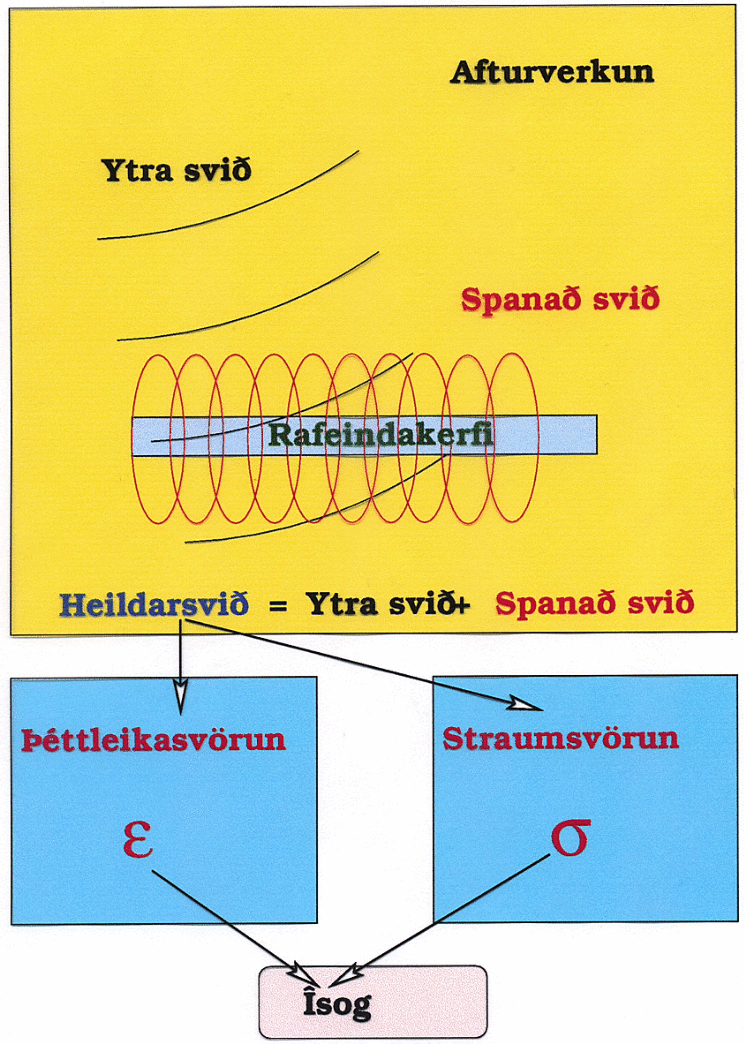

Þéttleiki rafeinda í kassalaga punkti

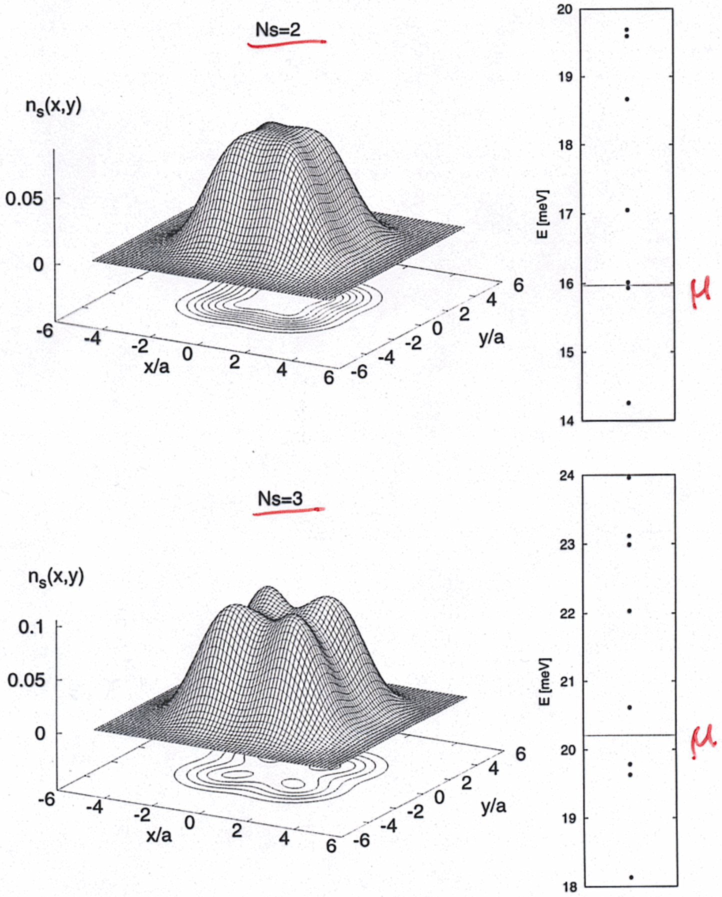

Figure 4.5: The density of two (above) and three (below) interacting electrons subject to a square symmetric confinement, $\alpha_1 = 0.0$ and $\alpha_2 = 0.4$. The magnetic length is $a = 13$ nm.

Spanaður þéttleiki vegna ísogs

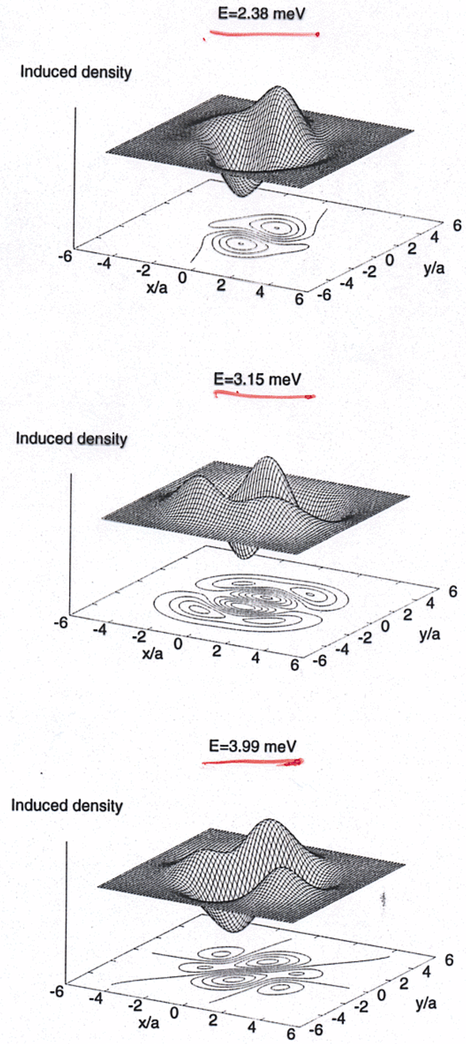

Figure 7.2: The induced density at the absorption peaks for $N_p = -1$. See discussion in text.

Innri hreyfingar

Skammtapunktur með gati í miðju

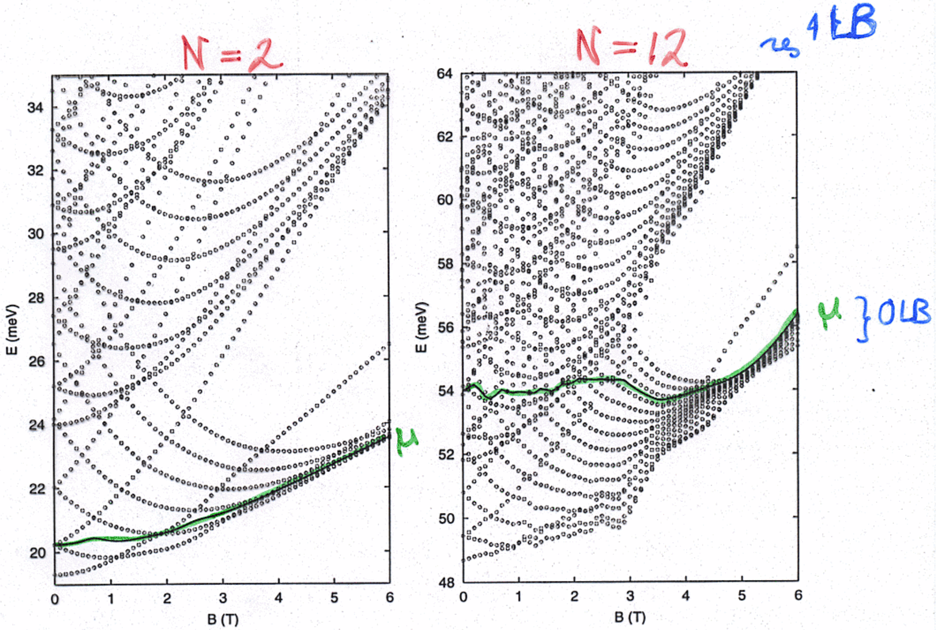

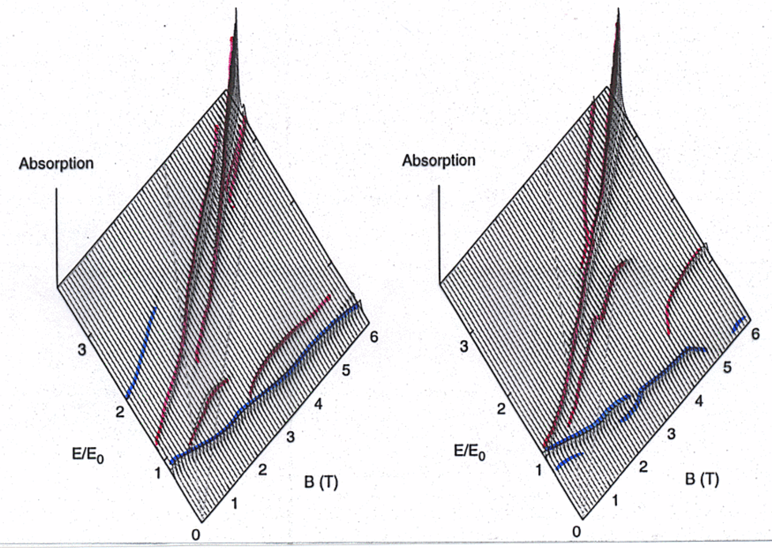

Klassísk hreyfing rafeinda borin saman við líkindadreif. þeirra samtv. skammtafr.

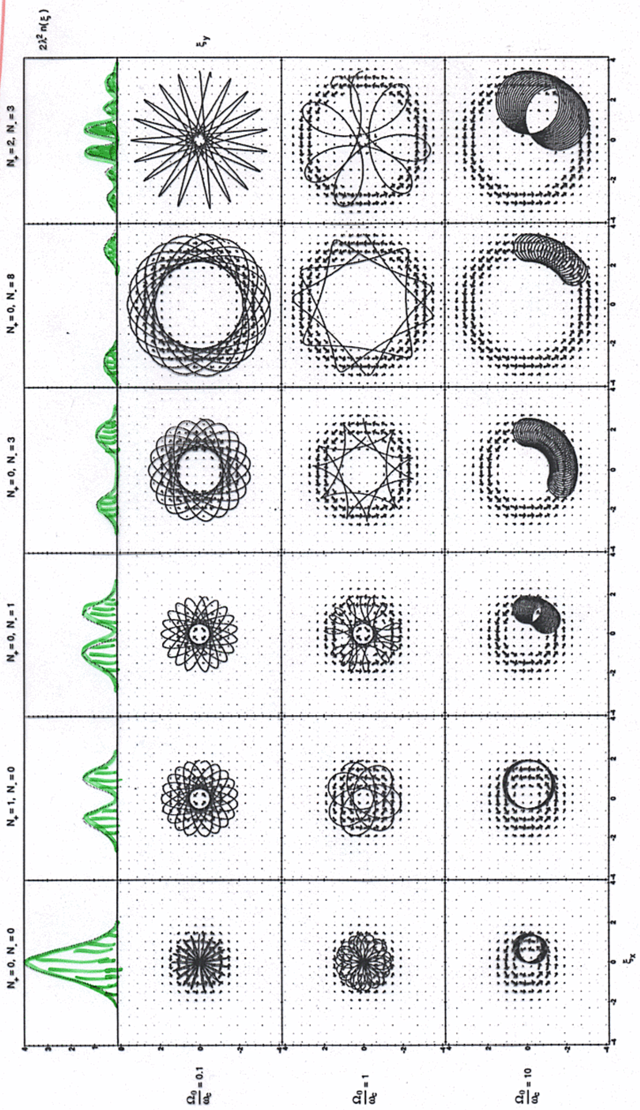

Fig. 4.4: Density (upper row) and current distribution (lower rows) in parabolic quantum dot states $|N_+, N_-\rangle$ at different ratio Ω_0/ω_c. Solid lines indicate corresponding classical orbits.

Rafeind í punkti

Seglun í 2DEG

Miðsæ kerfi

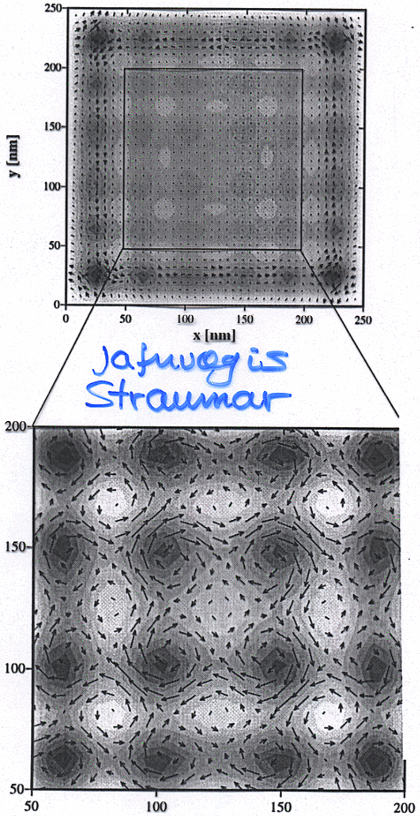

Jafnvægis Straumar

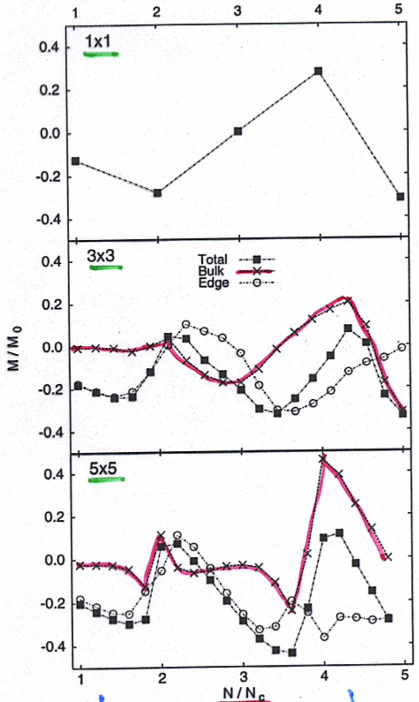

Lítið kerfi Stakkað

Jaðar

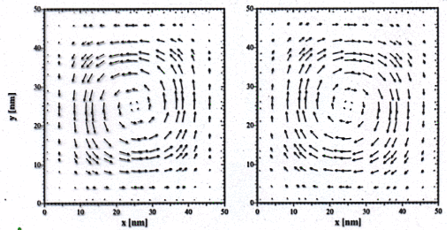

viðbót rafeinda
snýr seglun og
straumum við

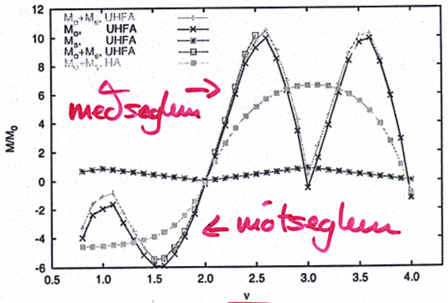

Óendanlega stórt
lotubundið kerfi

Rafeindir í lotubundnu tvívíðu kerfi

Kristallur

⋮

mótuð kerfi

Cond-mat 9509064

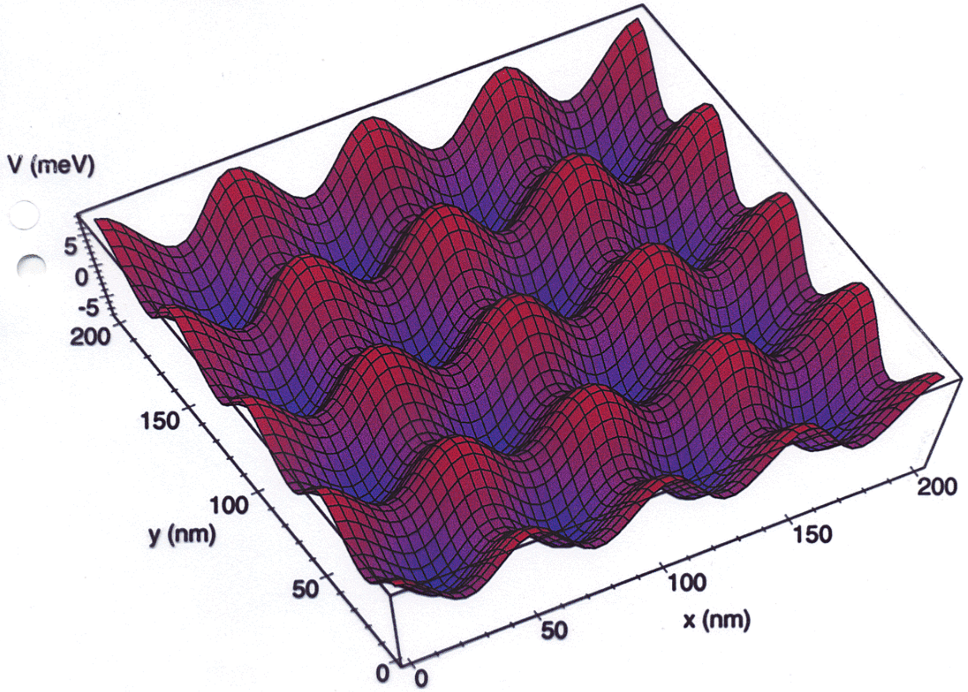

[redacted]

Víxlverkandi rafeindir í tvílotubundnu ytra mætti og þverstæðu einsleitu segulsviði $\vec{B}$

$\Downarrow$

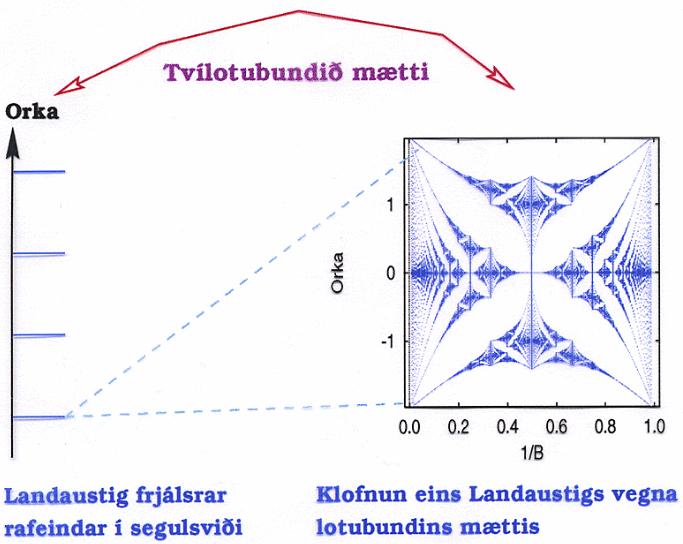

Fiðrildi Hofstadters $\leftrightarrow$ Grunnástand, ljósísog

Tilraunir í undirbúningi fyrir ljósísog

PHYSICAL REVIEW B VOLUME 14, NUMBER 6 15 SEPTEMBER 1976

Energy levels and wave functions of Bloch electrons in rational and irrational magnetic fields*

Douglas R. Hofstadter†
Physics Department, University of Oregon, Eugene, Oregon 97403
(Received 9 February 1976)

An effective single-band Hamiltonian representing a crystal electron in a uniform magnetic field is constructed from the tight-binding form of a Bloch band by replacing $\hbar\vec{k}$ by the operator $\vec{p} - e\vec{A}/c$. The resultant Schrödinger equation becomes a finite-difference equation whose eigenvalues can be computed by a matrix method. The magnetic flux which passes through a lattice cell, divided by a flux quantum, yields a

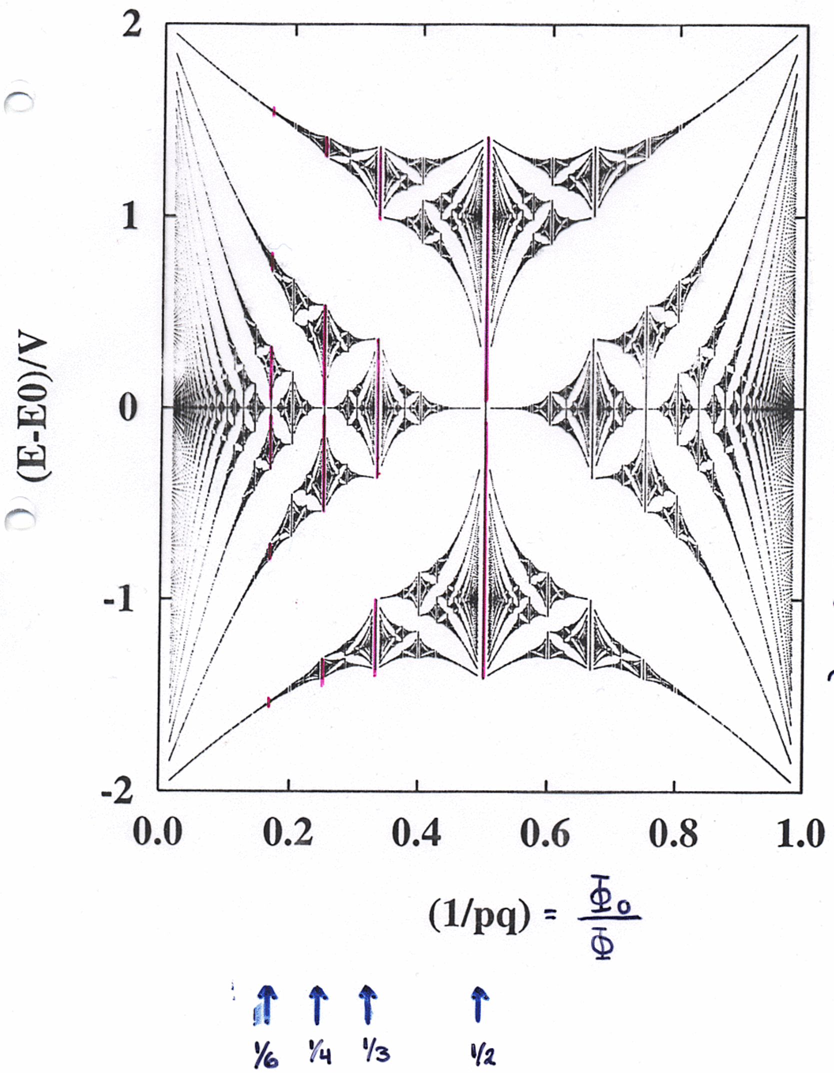

rational

finite number of Subbands

irrational

uncountably many levels with a gap between any pair

~ Cantor set

Samantekt ⇔ notkun

* smækkun rása, klassískt -> skammta
* smárar fyrir einstakar rafeindir, SET
* ljósnemar á fjarinnrauða sviðinu
* vélbúnaður fyrir „cellular automata"
* skammta tölvur
* Grunnrannsóknir

$$E_{tot} = E_{kin} + E_{direct}(n) + E_{xc} + E_{corr.}[\{\Psi\}]$$

PHYSICAL REVIEW VOLUME 136, NUMBER 3B 9 NOVEMBER 196

Inhomogeneous Electron Gas*

P. HOHENBERG†
École Normale Superieure, Paris, France
AND
W. KOHN‡
École Normale Superieure, Paris, France and Faculté des Sciences, Orsay, France
and
University of California at San Diego, La Jolla, California
(Received 18 June 1964)

This paper deals with the ground state of an interacting electron gas in an external potential $v(\mathbf{r})$. It is proved that there exists a universal functional of the density, $F[n(\mathbf{r})]$, independent of $v(\mathbf{r})$, such that the expression $E\equiv\int v(\mathbf{r})n(\mathbf{r})d\mathbf{r}+F[n(\mathbf{r})]$ has as its minimum value the correct ground-state energy associated with $v(\mathbf{r})$. The functional $F[n(\mathbf{r})]$ is then discussed for two situations: (1) $n(\mathbf{r})=n_0+\tilde{n}(\mathbf{r})$, $\tilde{n}/n_0\ll1$, and (2) $n(\mathbf{r})=\varphi(\mathbf{r}/r_0)$ with φ arbitrary and $r_0\to\infty$. In both cases F can be expressed entirely in terms of the correlation energy and linear and higher order electronic polarizabilities of a uniform electron gas. This approach also sheds some light on generalized Thomas-Fermi methods and their limitations. Some new extensions of these methods are presented.

PHYSICAL REVIEW VOLUME 140, NUMBER 4A 15 NOVEMBER 1965

Self-Consistent Equations Including Exchange and Correlation Effects*

W. KOHN AND L. J. SHAM
University of California, San Diego, La Jolla, California
(Received 21 June 1965)

From a theory of Hohenberg and Kohn, approximation methods for treating an inhomogeneous system of interacting electrons are developed. These methods are exact for systems of slowly varying or high density. For the ground state, they lead to self-consistent equations analogous to the Hartree and Hartree-Fock equations, respectively. In these equations the exchange and correlation portions of the chemical potential of a uniform electron gas appear as additional effective potentials. (The exchange portion of our effective potential differs from that due to Slater by a factor of $\frac{2}{3}$.) Electronic systems at finite temperatures and in magnetic fields are also treated by similar methods. An appendix deals with a further correction for systems with short-wavelength density oscillations.

Sama $E_{tot} = E_{tot}[n]$ DFT

ýmsar nálganir.... LDA.....

Í mikilli þróun